ISSN 0029 - 3865

CBPF-NF-059/84

SYSTEMATIC OF THE SLOPE-MASS-CORRELATIONS IN DIFFRACTIVE DISSOCIATION REACTIONS

by

A.C.B. Antunes*, A.F.S. Santoro
and M.H.G. Souza

Centro Brasileiro de Pesquisas Físicas - CBPF/CNPq
Rua Dr. Xavier Sigaud, 150
22290 - Rio de Janeiro, RJ - Brasil

*Instituto de Física
Universidade Federal do Rio de Janeiro
Caixa Postal 68528
21910 - Rio de Janeiro, RJ - Brasil

ABSTRACT

We present in this paper a set of several results of the Three Components Deck Model for Diffractive Dissociation Reactions. News and recently published results are summarized to obtain a general overview of the model, its predictions and comparison with experimental results. Two kinds of correlations and amplitudes are given: The slope-mass-cos θ^{GJ} correlation and slope-mass-partial wave.

Key-words: Diffraction; Dissociation; Correlation.

1 INTRODUCTION

One of the most important part of the high energy scattering is the inelastic Diffractive Component or Diffraction Dissociation. The Three Components Deck Model (TCDM) gives a very good description of the Diffractive Dissociation phenomena. We have published[1] a set of applications in several reactions with a very good result. Other applications will be presented here giving a certain universalisation to the model. Our aim in this review is summarize all known and new applications of the (TDCM) giving a general view of the main properties. For a general review about all diffractive aspects of the scattering see reference [2].

As the different aspects of the scattering, the Inelastic Diffractive part have also soft and hard components in physical regions. And while the soft component has been very much studied and good models exist, the hard component is a very unfamiliar part of the scattering. This is an open and interesting phenomenological and theoretical subject.

In this paper we stick ourselves at the Diffractive Dissociation soft component and specifically at the (TCDM)[1a]. We have shown that[1] this model reproduces the main aspects of the Diffractive Dissociation reactions (DDR). Here, we put together all new and published results for different reactions, giving a complete systematic of the spin-parity structure. The (TCDM) is the only model describing, (among the main properties of the data), the mass-slope-$\cos\theta^{G\bar{J}}$ and mass-slope-partial-wave correlations. A summary of the improvements, derivations, spin-parity structures for each reaction, approximations and hypothesis are given

in the next sections. The section II is dedicated to the model and the main aspects of it derivation. In the section III we give the applications of the (TCDM) to several reactions with different spin and parity structure in the $a + I\!P \to 1 + 2$ subreaction (where a is the beam-particle, $I\!P$ is the Pomeron exchanged in the complete inelastic reaction and (1 + 2) is the subsystem in which we study the effective mass distributions and general properties). Partial wave amplitudes for each reaction are given in section IV. And finally in section V we present the discussions and conclusions.

2 THREE COMPONENTS DECK MODEL

We present now the general description of the (TCDM) its properties and main parts of the derivation.

In all cases we have considered a general reaction $a + b \to (1 + 2) + 3$, see fig. (1), where b = 3 = Nucleon, at very high energy where the diffractive phenomena are dominant. In (TCDM) the Diffractive character is represented by the Pomeron ($I\!P$) exchange. The dissociation of the hadron (a) into a pair (1 + 2) is described by the coherent sum of the Born terms of the exchange amplitudes of the (a), (1) and (2) particles or the s, t and u channel respectively of the subreaction $a + I\!P \to 1 + 2$, see fig. (2). We use a standard parametrization of the Pomeron exchange, as we will see below. The two parameters b and σ_T^∞, the slope and the asymptotic total cross section are in general experimentally known. But in our case the subreac

tions: $(\underline{2}) + (b) \to (2) + (3=b), (\underline{1}) + (b) \to (1) + (3=b)$ and $(a) + (b) \to (\underline{a}) + (3=b)$ are off-mass-shell in the sense that $(\underline{2})$, $(\underline{1})$ and $(\underline{a})$ are off-mass-shell particles. Then we must correct the off-shell problem by changing slightly the b and σ_T^∞ in each case. This is the best form to consider indirectly a "form factor" without broke some other important properties as the interference among the three terms.

The well known Gribov-Morrison rule[3], $\Delta P = (-1)^{\Delta J}$, where ΔP and ΔJ are the Parity and spin balance between the particles in the diffractive vertex, is automatically satisfied in elastic diffractive subreactions, which appear in the TCDM.

To obtain the hadronic current coupled to the IPomeron, in the (TCDM), we assume the vector coupling hypothesis (VCH). On the current constructed with this hypothesis we must impose the s-channel helicity conservation (SCHC) which simplifies the form of the coupling, and reduces the coupling constants to only one. It is a well known experimental result that in the elastic diffractive reactions, dominated by the IPomeron exchange, the IPomeron couples only to the s-channel helicity conserving hadronic vertex[4].

In the High Energy Approximation (HEA), defined in Appendix A, the S-channel helicity conservated current, for a vertex á (p,λ) IPb(p',λ') obtained with (VCH), has the general form[5]

$$J^{\beta}_{\lambda',\lambda}(p',p) \simeq (-t)^{|\lambda'-\lambda|/2} V(\lambda',\lambda) P^{\beta} \qquad (1)$$

where $t = (p'-p)^2$, $P = (p'+p)/2$ and

$V(\lambda',\lambda)$)are functions of the coupling constants, the masses m_a, m_b and the momentum transfer t.

Imposing the SCHC on these currents they become[1d]

$$J^{\beta}_{\lambda',\lambda}(p',p) \simeq 2g_{a\mathbb{P}b}\, P^{\beta}\delta_{\lambda'\lambda} \tag{2}$$

In the diffractive region, dominated by the Pomeron exchange, the helicity amplitudes are essentially imaginary. For a generic diffractive reaction,

$$a(p,\lambda_a) + b(q,\lambda_b) \to a(p',\lambda'_a) + b(q',\lambda'_b)$$

the helicity amplitudes may be written as

$$A(s,t)_{\lambda_a,\lambda_b,\lambda'_a,\lambda'_b} = \frac{i}{2}\, e^{Bt/2} J_{\beta;\lambda'_a\lambda_a} J^{\beta}_{\lambda'_a\lambda_b} \tag{3}$$

The relation among the coupling constants, which appear in the currents, and the total cross section is given by the optical theorem

$$g_{aa\mathbb{P}}\, g_{bb\mathbb{P}} = \sigma^{ab}_{t_o t}(\infty) \tag{4}$$

Off mass shell corrections must be introduced in the diffractive amplitudes contained in the TCDM. It is important to emphasizes here the inconvenience of introducing form factors to take into account off mass shell effects. The complications due to the presence of form factors could destroy the possible interferences among the components of TCDM.

The most convenient way to introduce the off mass shell effects is via small variations of the experimental diffractive slopes (B_{2b}, B_{1b} and B_{ab}) and the cross sections values ($\sigma^{2b}_{Tot}(\infty)$, $\sigma^{1b}_{Tot}(\infty)$ and $\sigma^{ab}_{Tot}(\infty)$).

In the (HEA), the general form of the common vertex (b$\mathbb{P}$3), at the three components, considering that (b = 3), is given by

$$J^{\beta}_{\lambda_3\lambda_b} \simeq 2g_{b\mathbb{P}}R^{\beta}\delta_{\lambda_3\lambda_b} \tag{5}$$

where $R = (p_b + p_3)/2$.

The factorization property of the pomeron permits to factorize this common vertex in the TCDM. This factorization may be represented as in fig. (3).

A consequence of this property in the case of the (TCDM) is that the spins of the (b$\mathbb{P}$3) vertex do not affect the general structure of the (TCDM). Then, at the (HEA), the spins of the particles (b) and (3) may be neglected, and the current (5) may be written as

$$J^{\beta} \simeq 2g_{b\mathbb{P}}R^{\beta} \tag{6}$$

To materialize the problem and to introduce a standard notation for our applications of TCDM, let us consider a particular type of reaction in which the particle (b) = (3) is a nucleon and (a), (1) and (2) are spinless hadrons.

The amplitudes for each component of the TCDM, represented in fig. (2), with the kinematic defined in Appendix

A, are

$$A^{(t)} = \frac{i}{2} e^{B_{2b}t_2/2}(2g_{b\mathbb{P}}R^{\beta})(2g_{2\mathbb{P}}Q_{\beta})\frac{1}{t_1 - m_2^2} g_{a12} \qquad (7a)$$

$$A^{(u)} = \frac{i}{2} e^{B_{1b}t_2/2}(2g_{b\mathbb{P}}R^{\beta})(2g_{1\mathbb{P}}P_{\beta})\frac{1}{u_1 - m_1^2} g_{a12} \qquad (7b)$$

and

$$A^{(s)} = \frac{i}{2} e^{B_{ab}t_2/2}(2g_{b\mathbb{P}}R^{\beta})(2g_{a\mathbb{P}}K_{\beta})\frac{1}{s_1 - m_a^2} g_{a12} \qquad (7c)$$

To simplify these expressions we define

$$g^t(t_2) = \sigma_{tot}^{2b}(\infty)e^{B_{2b}t_2/2}$$

$$g^u(t_2) = \sigma_{tot}^{1b}(\infty)e^{B_{1b}t_2/2}$$

and

$$g^s(t_2) = \sigma_{tot}^{ab}(\infty)\, e^{B_{ab}t_2/2} \qquad (8)$$

where, according to (4), $\sigma_{tot}^{2b}(\infty) = g_{b\mathbb{P}}g_{2\mathbb{P}}$, $\sigma_{tot}^{1b}(\infty) = g_{b\mathbb{P}}g_{1\mathbb{P}}$ and $\sigma_{tot}^{ab}(\infty) = g_{b\mathbb{P}}g_{a\mathbb{P}}$, and also

$$T = ig_{a12}g^t(t_2)/(t_1 - m_2^2)$$

$$U = ig_{a12}g^u(t_2)/(u_1 - m_1^2)$$

and

$$S = ig_{a12}g^s(t_2)/(s_1 - m_a^2) \qquad (9)$$

At the HEA (A-9), using (A-10) and the definitons above, the components (7) become

$$A^{(t)} = T = s_2 . \mathcal{T}$$

$$A^{(u)} = U = s_3 . \mathcal{U}$$

and

$$A^{(s)} = S = s . \mathcal{S} \tag{10}$$

The scattering amplitude is the coherent sum of the three components, $A = A^{(s)} + A^{(t)} + A^{(u)}$. Then for reactions with spinless particles in the dissociative vertex, $\delta_a = \delta_1 = \delta_2 = 0$, the TCDM yields

$$A = S + T + U = ig_{a12}\left\{\frac{s . g^s(t_2)}{s_1 - m_a^2} + \frac{s_2 . g^t(t_2)}{t_1 - m_2^2} + \frac{s_3 . g^u(t_2)}{u_1 - m_1^2}\right\} \tag{11}$$

The general forms of the components, considering the spin factors, are $A^{(s)} = F^{(s)} . \mathcal{S}$, $A^{(t)} = F^{(t)} . \mathcal{T}$ and $A^{(u)} = F^{(u)} \mathcal{U}$, where $F^{(s)}$, $F^{(t)}$ and $F^{(u)}$ are functions of the masses and invariants (A - 3). It is clear that for spinless particles $F^{(s)} = s$, $F^{(t)} = s_2$ and $F^{(u)} = s_3$.

The components of the TCDM summed up coherently may interfere destructively in some kinematical regions. This interference is the mechanism which gives rise to the correlation among three variables: the diffractive slope (B), the effective mass ($M_{12} = \sqrt{s_1}$) of the dissociated system and the polar coordinate $(\theta)^{GJ}$ of a dissociated particle momentum ($\vec{p}_1$) relative to the incident beam momentum ($\vec{p}_a$) in the GJS.

Another feature of this correlation is the slope-mass-partial waves correlation, which will be studied in section IV. A direct consequence of the interferences above referred is the large slopes and/or the dips obtained in the $d\sigma/dt_2$ distributions.

In the spinless cases it is possible to obtain equations that give the positions of the dips and show clearly the correlation among M_{12}, $\cos\theta^{G.J.}$ and t_2.

At (HEA) $s \simeq s_2 + s_3$, carring this into the equation (11) and making equal to zero the coefficients of s_2 and s_3, we obtain,

$$Z_{st} \equiv g^s(t_2)(t_1 - m_2^2) + g^t(t_2)(s_1 - m_a^2) = 0$$

$$Z_{su} \equiv g^s(t_2)(u_1 - m_1^2) + g^u(t_2)(s_1 - m_a^2) = 0 \qquad (12)$$

Some observations may be done on these equations:

a) They may be satisfied in the physical region since in this region $s_1 - m_a^2$ is positive whereas $t_1 - m_2^2$ and $u_1 - m_1^2$ are negative.

b) They may be rewritten as

$$\cos\theta^{GJ} = f_1(t_2) \quad ; \quad M_{12} = f_2(t_2) \qquad (13)$$

which show clearly the correlation, among the three variables M_{12}, $\cos\theta^{GJ}$ and t_2, predicted by this model.

c) The factorization of the elastic vertex (bP3) in the TCDM, according to fig. (3), shows that the position (M_{12}, $\cos\theta^{GJ}$, t_2) of the zero in the amplitude, or of the dip in $d\sigma/dt_2$,

is independent of the hadron (b).

d) The parameters that fix the position of the zeros of the amplitudes are the total asymptotic cross sections $\sigma_{tot}^{ib}(\infty)$ and the elastic slopes B_{ib} (i = a,1,2).

Dual Reggeization of TCDM

In the present form of the TCDM, each component is the Born term of the amplitudes of exchange of the particles (a), (1) and (2). The validity of the model is restricted to the effective mass ($M_{12} = \sqrt{s_1}$) range between the threshold and the resonances of the dissociated subsystem (1 + 2).

The need for reggeization has been finding out since the beginning of the DDR fenomenology development.

The reggeization of the TCDM must be done with some care. The components of exchange of particles (a), (1) and (2) must be handled in a symmetric way, because the interferences that generate the slope-mass-$\cos\theta^{GJ}$ correlation must not be lost in the course of the process.

The solution of this problem is given by duality. Duality supplies a Regge behaviour to the three channels, avoiding double counting and dealing with all the channels in a symmetric way[1a].

The procedure for dual reggeization of the TCDM, in the spinless case has been performed in reference[1a] using Veneziano formula,

$$A = ig_{a12}\left\{s_3^{Z_{su}}\frac{\Gamma(-\alpha_s)\Gamma(-\alpha_u)}{\Gamma(1-\alpha_s-\alpha_u)} + s_2^{Z_{st}}\frac{\Gamma(-\alpha_s)\Gamma(-\alpha_t)}{\Gamma(1-\alpha_s-\alpha_t)}\right\} \quad ,(14)$$

where

$$\alpha_s = s_1 - m_a^2,\ \alpha_t = t_t - m_2^2 \quad \text{and} \quad \alpha_u = u_1 - m_1^2.$$

3 APPLICATIONS OF TCDM TO SEVERAL TYPES OF DDR.

In this section we collect several results of TCDM applications. The DDR studied here have different configurations of spin and parity in the dissociative vertex $(a \to 1 + 2)$. These configurations will be denoted as $(\delta_a^P \to \delta_1^P, \delta_2^P)$.

The following configurations are analysed here:

$$A - (0^- \to 0^+, 0^-);\ B - (0^- \to 1^-, 0^-);\ C - (1/2^+ \to 1/2^+, 0^-);$$

and $$D - (1/2^+ \to 3/2^+, 0^-).$$

Some examples of reactions that correspond to these structures of spin and parity are:

$$A - \pi + p \to (\varepsilon + \pi) + p;\ K + p \to (\kappa + \pi) + p;$$

$$B - \pi + p \to (\rho^0 + \pi) + p;\ K + p \to (K^* + \pi) + p;$$

$$C - p + p \to (n + \pi^+) + p;\ p + p \to (\Lambda + K^+) + p;$$

$$D - p + p \to (\Delta^{++} + \pi^-) + p$$

The TCDM amplitudes for DDR of type A have already been obtained in the precedent section.

For reactions of type B, the components of TCDM are, using the kinematics of appendix A:

$$A^{(t)}_{\lambda_1} = \frac{i}{2}\, e^{B_{b2}t_2/2}(2g_{b\mathbb{P}}R^{\beta})(2g_{2\mathbb{P}}Q_{\beta})\frac{1}{t_1 - m_2^2}\, g_{a12}\varepsilon^{*}_{u}(p_1,\lambda_1)p_a^{\mu}\ ,$$

$$A^{(s)}_{\lambda_1} = \frac{i}{2}\, e^{B_{ab}t_2/2}(2g_{b\mathbb{P}}R^{\beta})(2g_{a\mathbb{P}}K_{\beta})\frac{1}{s_1 - m_a^2}\, g_{a12}\varepsilon^{*}_{\mu}(p_1,\lambda_1)p_2^{\mu}\ ,$$

$$A^{(u)}_{\lambda_1} = \frac{i}{2}\, e^{B_{1b}t_2/2}(2g_{b\mathbb{P}}R_{\beta})\varepsilon^{*}_{\mu}(p_1,\lambda_1)\Gamma^{\mu\beta\nu}\frac{(-g_{\nu\sigma}+k_{\nu}k_{\sigma}/k^2)}{u_1 - m_1^2}\, g_{a12}(p_a+p_2)^{\sigma}/2, \tag{15}$$

where $\varepsilon_{\mu}(p_1,\lambda_1)$ is the wave function for spin 1 particles and

$$\Gamma^{\mu\beta\nu} = 2g_{1\mathbb{P}}\left[2(g^{\mu\beta}p^{\nu} + p^{\mu}g^{\beta\nu}) - g^{\mu\nu}p^{\beta}\right] \tag{16}$$

is the s - channel helicity conserving coupling in the vertex $(1^{-}\mathbb{P}1^{-})$.

In the HEA, and using the notation introduced in section II, those components may be written as

$$A^{(t)}_{\lambda_1} \simeq T\,\varepsilon^{*}_{\mu}(p_1,\lambda_1)p_a^{\mu}\ ,$$

$$A^{(s)}_{\lambda_1} \simeq S\,\varepsilon^{*}_{\mu}(p_1,\lambda_1)p_2^{\mu}$$

and

$$A^{(u)}_{\lambda_1} \simeq \left[Up_a^{\mu} + s\,U(p^{\mu} - p_a^{\mu}) - U.R^{\mu}(s_1 + m_a^2 - m_2^2 - t_1)/4\right]\varepsilon^{*}_{\mu}(p_1,\lambda_1) \tag{17}$$

In the G.J.S. we have

$$p_a^{\mu} = E_a E^{\mu} + |\vec{p}_a|\, Z^{\mu} \quad \text{and} \quad p^{\mu} = \sqrt{s_1}\, E^{\mu} \tag{18}$$

and at HEA

$$R^{\mu} \simeq \frac{s}{2\sqrt{s_1}}(E^{\mu} + \text{sen}\,\alpha\, X^{\mu} + \cos\,\alpha\, Z^{\mu}) \qquad (19)$$

where

$$E^{\mu} = \begin{pmatrix} 1 \\ 0 \\ 0 \\ 0 \end{pmatrix}, \quad X^{\mu} = \begin{pmatrix} 0 \\ 1 \\ 0 \\ 0 \end{pmatrix} \quad \text{and} \quad Z^{\mu} = \begin{pmatrix} 0 \\ 0 \\ 0 \\ 1 \end{pmatrix} \qquad (20)$$

Carring these results into expressions (17) and summing up the components, the helicity amplitudes read

$$A_{\lambda_1} = \left\{\sqrt{s_1}\, S + E_a T + E_a U + s\,U\,(m_1^2 + m_2^2 - \right.$$

$$\left. - m_a^2 + t_2 - u_1)/4\sqrt{s_1}\right\} \varepsilon_{\mu}^{*}(p_1, \lambda_1) E^{\mu} + \left\{s_2 |\vec{p}_a| T + \right.$$

$$\left. + s\,U \left[|\vec{p}_a| - (s_1 + m_a^2 - m_2^2 - t_1)\cos\alpha/4\sqrt{s_1}\right]\right\} \varepsilon_{\mu}^{*}(p_1, \lambda_1) Z^{\mu} -$$

$$- \left[s\,U\,(s_1 + m_a^2 - m_2^2 - t_1)\,\text{sen}\,\alpha/4\sqrt{s_1}\right] \varepsilon_{\mu}^{*}(p_1 \lambda_1) X^{\mu} \,. \qquad (21)$$

The spin 1 wave functions are

$$\varepsilon^{\mu *}(p_1, 0) = \frac{1}{m_1}\begin{pmatrix} p_1 \\ E_1 \sin\theta\, \cos\phi \\ E_1 \sin\theta\, \text{sen}\,\phi \\ E_1 \cos\theta \end{pmatrix}, \quad \varepsilon^{\mu *}(p_1, \pm 1) = \frac{e^{\mp i\phi}}{\sqrt{2}}\begin{pmatrix} 0 \\ \mp\cos\theta\, \cos\phi - i \sin\phi \\ \mp\cos\theta\, \sin\phi + i \cos\phi \\ \pm\sin\theta \end{pmatrix} \qquad (22)$$

and the helicity amplitudes (21) are explicitly :

$$A_{\lambda_1=0} = |\vec{p}_1|\left\{\sqrt{s_1}\,S + E_a T + E_a U + s\,U\,(m_1^2 + m_2^2 - m_a^2 + \right.$$

$$\left. + t_2 - \mu_1)/4\sqrt{s_1}\right\}/m_1 - E_1\left\{s_2|\vec{p}_a|\,T + s\,U\left[|\vec{p}_a| - (s_1 + \right.\right.$$

$$\left.\left. m_a^2 - m_2^2 - t_1)\cos\alpha/4\sqrt{s_1}\right]\right\}\cos\theta/m_1 - s\,U\,E_1(s_1 + m_a^2 -$$

$$- m_2^2 - t_1)\sin\alpha\,\mathrm{sen}\,\theta\,\cos\phi/(4m_1\sqrt{s_1}) \quad , \tag{23}$$

and

$$A_{\lambda_1=\pm1} = \mp\, e^{\mp i\phi}\left\{\left\{s_2|\vec{p}_a|\,T + s\,U\left[|\vec{p}_a| - (s_1 + m_a^2 - m_2^2 - \right.\right.\right.$$

$$\left.\left.\left. - t_1)\cos\alpha/4\sqrt{s_1}\right]\right\}\sin\theta - s\,U\,(s_1 + m_a^2 - m_2^2 -\right.$$

$$\left. - t_1)\sin\alpha(\cos\theta\,\cos\phi \pm i\sin\phi)/4\sqrt{s_1}\right\}/\sqrt{2} \ . \tag{24}$$

The possible zeros in these amplitudes may not be determined by simple equations like that for spinless reactions. In this case they must be sought numerically.

Reactions of type C have the following components for the TCDM:

$$A^{(t)}_{\lambda_1\lambda_a} = 2T\,R.Q\bar{u}(p_1,\lambda_1)\gamma_5 u(p_a,\lambda_a)$$

$$A^{(u)}_{\lambda_1\lambda_a} = U\,\bar{u}(p_1,\lambda_1)\not{R}(\not{K} + m_1)\gamma_5 u(p_a,\lambda_a)$$

and

$$A^{(s)}_{\lambda_1\lambda_a} = S\,\bar{u}(p_1,\lambda_1)\gamma_5(\not{p} + m_a)\not{R}u(p_a,\lambda_a) \ . \tag{25}$$

The helicity amplitudes, obtained summing these components, may be written as

$$A_{\lambda_1\lambda_a} = R_\beta \bar{u}(p_1\lambda_1)\left\{2(T+S)p_2^\beta\gamma_5 - (U+S)\gamma^\beta \not{p}_2\gamma_5\right\} u(p_a,\lambda_a) \quad (26)$$

where we have assumed $m_1 = m_a$.

It may occur zeros in these amplitudes, due to interferences among the components, if

$$T + S = 0 \quad \text{and} \quad U + S = 0 \quad (27)$$

in the physical region. The equations for the zeros are

$$Z_{st} = (s_1 - m_a^2)g^t(t_2) + (t_1 - m_2^2)g^s(t_2) = 0$$

$$Z_{su} = (s_1 - m_a^2)g^u(t_2) + (u_1 - m_1^2)g^s(t_2) = 0 \quad (28)$$

These equations are the same as that obtained for spinless reactions (12).

For the reaction $pp \to n\pi p, ^1a$, from eqs. (28) and using the relation $s_1 + t_1 + u_1 = 2m_N^2 + m_\pi^2 + t_2$, we obtain

$$t_{1(dip)} = m_\pi^2 + t_2$$

and

$$s_{1(dip)} = m_N^2 - t_2 \cdot e^{\Delta \cdot t_2} \cdot \delta \quad , \quad (29)$$

where

$$\delta = \sigma_{NN}/\sigma_{\pi N} \quad \text{and} \quad \Delta = (B_{NN} - B_{\pi N})/2.$$

These equations describe correctly the behaviour of the zero in the amplitudes, or the dip in $d\sigma/dt_2$.

The helicity amplitudes for this type of reaction may be written in a form more convenient for calculations. Summing the components (25), in the HEA, we obtain

$$A_{\lambda_1\lambda_a} = (S + T + U)\bar{u}(p_1\lambda_1)\gamma_5 u(p_a\lambda_a) - i s|\vec{p}_a|(U+S)\sin\alpha\,\bar{u}(p_1\lambda_1)(\sigma^{31} -$$

$$- \cos\alpha\,\sigma^{01} + \sin\alpha\,\sigma^{03})\gamma_5 u(p_a\lambda_a)/2\sqrt{s_1}\,. \qquad (30)$$

This gives explicitly:

$$A_{\pm 1/2,\pm 1/2} = \pm\left\{(S + T + U)G_-\cos(\theta/2) - \right.$$

$$- s|\vec{p}_a|(S+U)\sin\alpha\left[E_+\sin\alpha\cos(\theta/2) - e^{\mp i\phi}(G_+ +\right.$$

$$\left.\left. + E_+\cos\alpha)\sin(\theta/2)\right]/2\sqrt{s_1}\right\}\,. \qquad (31)$$

and

$$A_{\mp 1/2,\pm 1/2} = -e^{\pm i\phi}\left\{(S + T + U)G_+\sin(\theta/2) + \right.$$

$$+ s|\vec{p}_a|(S+U)\sin\alpha\left[E_-\sin\alpha\sin(\theta/2) - e^{\mp i\Phi}(G_- +\right.$$

$$\left.\left. + E_-\cos\alpha)\cos(\theta/2)\right]/2\sqrt{s_1}\right\}\,, \qquad (32)$$

where

$$E_{\pm} = (E_1 + m_1)^{1/2}(E_a + m_a)^{1/2} \pm (E_1 - m_1)^{1/2}(E_a - m_a)^{1/2}$$

$$G_{\pm} = (E_1 + m_1)^{1/2}(E_a - m_a)^{1/2} \pm (E_1 - m_1)^{1/2}(E_a + m_a)^{1/2} \tag{33}$$

Dual Resonance Parametrization

The TCDM for the reactions of type C may be reggeized and dualized. The helicity amplitudes (26) may be written as

$$A_{\lambda_1\lambda_a} = \bar{u}(p_1\lambda_1)\left\{\frac{2R.p_2 Z_{st}\gamma_5}{(s_1-m_a^2)(t_1-m_2^2)} - \frac{Z_{su}\not{R}\not{p}_2\gamma_5}{(s_1-m_a^2)(u_1-m_1^2)}\right\}u(p_a,\lambda_a). \tag{34}$$

The prescription for dual resonance parametrization (DRP) consists in substitute in eq. (34)

$$1/(s_1-m_a^2)(t_1-m_2^2) \quad \text{by} \quad \frac{\Gamma(-\alpha_a(s_1))\Gamma(-\alpha_2(t_1))}{\Gamma(1-\alpha_a(s_1)-\alpha_2(t_1))} \tag{35}$$

and

$$1/(s_1-m_a^2)(u_1-m_1^2) \quad \text{by} \quad \frac{\Gamma(-\alpha_a(s_1))\Gamma(-\alpha_1(u_1))}{\Gamma(1-\alpha_a(s_1)-\alpha_1(u_1))}\ . \tag{36}$$

The Regge trajectories are parametrized as

$$\alpha_1(u_1) = u_1 - m_1^2\ ,\ \alpha_2(t_1) = t_1 - m_2^2$$

and

$$\alpha_a(s_1) = s_1 - m_a^2 + i\lambda.(s_1 - (m_1 + m_2)^2)^{1/2}\ , \tag{37}$$

where the parameter λ controls the resonance width.

The TCDM has been applied to the reaction $pp \to \Delta^{++}\pi^-p$, which is of type D. Its components are

$$A^{(t)}_{\lambda_1\lambda_a} = 2R.QT\bar{\psi}_\mu(p_1,\lambda_1)p_a^\mu u(p_a,\lambda_a)$$

$$A^{(s)}_{\lambda_1\lambda_a} = S\bar{\psi}_\mu(p_1,\lambda_1)p_2^\mu(\not{p} + m_a)\not{K}u(p_a,\lambda_a)$$

and

$$A^{(u)}_{\lambda_1\lambda_a} = -U\bar{\psi}_\mu(p_1,\lambda_1)R_\beta\Gamma^{\mu\beta\nu}(m_1 + \not{K})\Lambda_{\nu\sigma}(k)p_2^\sigma u(p_a,\lambda_a) \quad (38)$$

where

$$\Gamma^{\mu\beta\nu} = g^{\mu\nu}(\gamma^\beta - 2P^\beta/m_1) + 4(g^{\mu\beta}P^\nu + P^\mu g^{\beta\nu})/m_1 \quad (39)$$

which is the coupling in the vertex $(3/2^+ \text{IP} 3/2^+)$ that assures the (SCHC) in this vertex, and

$$\Lambda_{\nu\sigma}(k) = g_{\nu\sigma} - 2k_\nu k_\sigma/3m_1^2 - \gamma_\nu\gamma_\sigma/3 + (k_\nu\gamma_\sigma - k_\sigma\gamma_\nu)/3m_1 \quad (40)$$

Summing up these components, in the (HEA), we have the following helicity amplitudes

$$A_{\pm 3/2,\pm 1/2} = \pm\frac{e^{\mp i\phi}}{\sqrt{2}}\Big\{s_3\,U(1+\frac{m_a}{m_1})|\vec{p}_a|E_-\sin\theta\cos(\theta/2) +$$

$$+ s_2|\vec{p}_a|\Big[((2+\frac{m_a}{m_1})E_- - \frac{\sqrt{s_1}}{m_1}E_+)\,U - E_-T\Big]\sin\theta\cos(\theta/2) +$$

$$+ \frac{s}{2}U(\frac{F_1}{\sqrt{s_1}}E_- + \frac{F_2}{m_1}E_+)\cos(\theta/2)\Big[\sin\alpha(\cos\theta\cos\phi \pm i\sin\phi) +$$

$$+ \cos\alpha\sin\theta\Big] - sU((m_1+m_a)^2 - m_2^2)|\vec{p}_a|\sin\theta\Big[E_+\cos(\theta/2) -$$

$$- G_+\sin\alpha\sin(\theta/2)e^{\mp i\phi} - G_+\cos\alpha\cos(\theta/2)\Big]/(2m_1\sqrt{s_1}) -$$

$$- s\,U\,(m_a + m_1)\,|\vec{p}_a|^2 \sin\alpha \sin\theta \left[G_- \sin\alpha \cos(\theta/2) + \right.$$

$$\left. + (E_- - G_- \cos\alpha) \sin(\theta/2) e^{\mp i\phi} \right] / (6 m_1 \sqrt{s_1}) \Bigg\} \qquad (41)$$

$$A_{\mp 3/2, \pm 1/2} = \frac{e^{\pm i 2\phi}}{\sqrt{2}} \Bigg\{ s_3\, U\, (1 + \frac{m_a}{m_1}) |\vec{p}_a|\, E_- \sin\theta \sin(\theta/2) +$$

$$+ s_2 |\vec{p}_a| \left[((2 + \frac{m_a}{m_1}) E_+ - \frac{\sqrt{s_1}}{m_1} E_-)\, U - E_+ T \right] \sin\theta \sin(\theta/2) +$$

$$\frac{s}{2} U \left(\frac{F_1}{\sqrt{s_1}} E_+ + \frac{F_2}{m_1} E_- \right) \sin(\theta/2) \left[\sin\alpha (\cos\theta \cos\phi \mp i \sin\phi) + \right.$$

$$\left. + \cos\alpha \sin\theta \right] - s\,U\,((m_1 + m_a)^2 - m_2^2) |\vec{p}_a| \sin\theta \left[E_- \operatorname{sen}(\theta/2) + \right.$$

$$\left. + G_- \sin\alpha \cos(\theta/2) e^{\mp i\phi} - G_- \cos\alpha \sin(\theta/2) \right] / (2 m_1 \sqrt{s_1}) -$$

$$- s\,U\,(m_a + m_1) |\vec{p}_a|^2 \sin\alpha \operatorname{sen}\theta \left[G_+ \sin\alpha \sin(\theta/2) - \right.$$

$$\left. - (E_+ - G_+ \cos\alpha) \cos(\theta/2) e^{\mp i\phi} \right] / (6 m_1 \sqrt{s_1}) \Bigg\} \qquad (42)$$

$$A_{\pm 1/2, \pm 1/2} = \sqrt{\frac{2}{3}} \frac{|\vec{p}_1|}{m_1} \left[\sqrt{s_1}\, E_- (s_3 S + s_2 T) ((1 + \frac{m_a}{m_1})(2\sqrt{s_1} - E_a) E_- - \right.$$

$$\left. - \frac{s_1}{m_1} E_+) s_3 U \right] \cos(\theta/2) + s_3\, U (1 + \frac{m_a}{m_1}) |\vec{p}_a| \left[\sqrt{\frac{2}{3}} \frac{E_1}{m_1} E_- \cos\theta \cos(\theta/2) - \right.$$

$$\left. - \frac{E_+}{\sqrt{6}} \sin\theta \sin(\theta/2) \right] + \sqrt{\frac{2}{3}} \frac{s_2}{m_1} \left[(\sqrt{s_1} - E_a) |\vec{p}_1| + |\vec{p}_a| E_1 \cos\theta \right] \times$$

$$\times \left[((2 + \frac{m_a}{m_1}) E_- - \frac{\sqrt{s_1}}{m_1} E_+)\, U - E_- T \right] \cos(\theta/2) -$$

$$- \frac{s_2}{\sqrt{6}} |\vec{p}_a| \left[((2 + \frac{m_a}{m_1}) E_+ - \frac{\sqrt{s_1}}{m_1} E_-)\, U - E_+ T \right] \operatorname{sen}\theta \sin(\theta/2) -$$

$$-\frac{s\,U}{\sqrt{6}\,m_1}\left(\frac{F_1}{\sqrt{s_1}}E_- + \frac{F_2}{m_1}E_+\right)\cos(\theta/2)\left[|\vec{p}_1| + E_1(\text{sen}\,\alpha\sin\theta\cos\phi - \right.$$

$$\left. - \cos\alpha\cos\theta)\right] - \frac{s\,U}{2\sqrt{6}}\left(\frac{F_1}{\sqrt{s_1}}E_+ + \frac{F_2}{m_1}E_-\right)\text{sen}(\theta/2)\left[\sin\alpha(\cos\theta\cos\phi \pm \right.$$

$$\left. \pm i\sin\phi) + \cos\alpha\sin\theta\right] - s\,U\,(m_1+m_a)^2 - m_2^2)\left((\sqrt{s_1} - E_a)|\vec{p}_1| + \right.$$

$$\left. + E_1|\vec{p}_a|\cos\theta\right)\left[E_+\cos(\theta/2) - G_+\sin\alpha\sin(\theta/2)e^{\mp i\phi} - \right.$$

$$\left. - G_+\cos\alpha\cos(\theta/2)\right]/(\sqrt{6s_1}\,m_1^2) + s\,U\,((m_1+m_a)^2 - m_2^2)|\vec{p}_a|\sin\theta\;x$$

$$x\left[E_-.\sin(\theta/2) + G_-\sin\alpha\cos(\theta/2)e^{\mp i\phi} - G_-\cos\alpha\sin(\theta/2)\right]/(2\sqrt{6s_1}\,m_1) +$$

$$+\sqrt{2}\,s|\vec{p}_a|\left[(((2m_1 - m_a)\,U - 3m_1 S)\sqrt{s_1} + (m_a + m_1)E_a\,U)|\vec{p}_1| - \right.$$

$$\left. - (m_1 + m_a)E_1|\vec{p}_a|\,U\cos\theta\right]\left[G_-\sin\alpha\cos(\theta/2) + (E_- - G_-\cos\alpha)\,x\right.$$

$$\left. x\sin(\theta/2)e^{\mp i\phi}\right]\sin\alpha/(6m_1^2\sqrt{3s_1}) + s\,U\,(m_a + m_1)|\vec{p}_a|^2\;x$$

$$x\sin\alpha\sin\theta\left[G_+\sin\alpha\sin(\theta/2) - (E_+ - G_+\cos\alpha)\;x\right.$$

$$\left. x\cos(\theta/2)e^{\mp i\phi}\right]/(6\sqrt{6s_1}\,m_1)\quad . \qquad (43)$$

$$A_{\mp 1/2,\pm 1/2} = \mp\, e^{\pm i\phi}\left\{\sqrt{\frac{2}{3}}\frac{|\vec{p}_1|}{m_1}\left[\sqrt{s_1}\,E_+(s\,S + s_2\,T) + \left((1+\frac{m_a}{m_1})(2\sqrt{s_1} - E_a)E_+ - \right.\right.\right.$$

$$\left.\left.\left. - \frac{s_1}{m_1}E_-\right)s_3\,U\right]\sin(\theta/2) + s_3\,U\,(1+\frac{m_a}{m_1})|\vec{p}_a|\left[\sqrt{\frac{2}{3}}\frac{E_1}{m_1}E_+\cos\theta\sin(\theta/2) + \right.$$

$$\left. + \frac{E_-}{\sqrt{6}}\sin\theta\cos(\theta/2)\right] + \sqrt{\frac{2}{3}}\frac{s_2}{m_1}\left[(\sqrt{s_1} - E_a)|\vec{p}_1| + |\vec{p}_a|E_1\cos\theta\right]\left[\left((2+\frac{m_a}{m_1})E_+ - \right.\right.$$

$$\left.\left. - \frac{\sqrt{s_1}}{m_1}E_-\right)U - E_+T\right]\sin(\theta/2) + \frac{s_2}{\sqrt{6}}|\vec{p}_a|\left[\left((2+\frac{m_a}{m_1})E_- - \frac{\sqrt{s_1}}{m_1}E_+\right)U - \right.$$

$$-E_{-}T\Big]\sin\theta\cos(\theta/2) - \frac{s\,U}{\sqrt{6}\,m_1}\Big(\frac{F_1}{\sqrt{s_1}}E_{+} + \frac{F_2}{m_1}E_{-}\Big)\sin(\theta/2)\Big[|\vec{p}_1| +$$

$$+E_1(\sin\alpha\sin\theta\cos\phi - \cos\alpha\cos\theta)\Big] + \frac{s\,U}{2\sqrt{6}}\Big(\frac{F_1}{\sqrt{s_1}}E_{-} + \frac{F_2}{m_1}E_{+}\Big)\cos(\theta/2)\,x$$

$$x\Big[\sin\alpha(\cos\theta\cos\phi \mp i\sin\phi) + \cos\alpha\sin\theta\Big] - s\,U\,((m_1+m_a)^2 - m_2^2)\;x$$

$$x\,((\sqrt{s_1} - E_a)|\vec{p}_1| + E_1|\vec{p}_a|\cos\theta)\Big[E_{-}\sin(\theta/2) + G_{-}\sin\alpha\cos(\theta/2)e^{\mp i\phi} -$$

$$- G_{-}\cos\alpha\sin(\theta/2)\Big]/(\sqrt{6s_1}\,m_1^2) - s\,U((m_1+m_a)^2 - m_2^2)|\vec{p}_a|\sin\theta\;x$$

$$x\Big[E_{+}\cos(\theta/2) - G_{+}\sin\alpha\sin(\theta/2)e^{\mp i\phi} - G_{+}\cos\alpha\cos(\theta/2)\Big]/(2\sqrt{6s_1}\,m_1) +$$

$$+\sqrt{2}\,s|\vec{p}_a|\Big[(((2m_1 - m_a)U - 3m_1 S)\sqrt{s_1} + (m_a + m_1)E_a U)|\vec{p}_1| -$$

$$-(m_1 + m_a)E_1|\vec{p}_a|\,U\cos\theta\Big]\Big[G_{+}\sin\alpha\sin(\theta/2) - (E_{+} - G_{-}\cos\alpha)\;x$$

$$x\cos(\theta/2)e^{\mp i\phi}\Big]\sin\alpha/(6m_1^2\sqrt{3s_1}) - s\,U(m_a + m_1)|\vec{p}_a|^2\;x$$

$$x\sin\alpha\sin\theta\Big[G_{-}\sin\alpha\cos(\theta/2) + (E_{-} - G_{-}\cos\alpha)\;x$$

$$x\sin(\theta/2)e^{\mp i\phi}\Big]/(6\sqrt{6s_1}\,m_1)\Big\} \quad . \tag{44}$$

where

$$F_1 = \Big\{3(2m_1 + m_a)(s_1 - u_1 - m_1^2 - 2m_2^2 + m_a^2)/m_1 + 2(m_1^2 + m_1 m_a +$$

$$+ m_a^2 - u_1) + m_a(m_a^2 - m_2^2 - u_1)/m_1 - (2m_1 + m_a)(m_a^2 - m_2^2 -$$

$$- u_1)(3u_1 + m_1^2 - t_2)/m_1^3 + (3u_1 + m_1^2 - t_2)(m_a^2 - u_1 - m_1^2 +$$

$$+ m_1 m_a)/m_1^2 - (2u_1 + 2m_1^2 - t_2)(m_a^2 - m_2^2 - u_1 - 2m_1^2)m_1^2 \Big\}/3 \ .$$

and

$$F_2 = \Big\{2t_2 - 2m_1 m_a + 5m_2^2 - 4m_a^2 - 3s_1 - 3m_1^2 + (3u_1 + m_1^2 -$$

$$t_2)(m_1^2 - m_1 m_a + m_a^2 - m_2^2 - u_1)/m_1^2 \Big\}/3. \qquad (45)$$

4 PARTIAL WAVE AMPLITUDES

In this section we project the helicity amplitudes, obtained in section III, into partial waves.

For reactions of type A, $(0^- \to 0^+, 0^-)$, the partial wave amplitudes are given by the eq. (B - 5), for $\lambda_a = 0$ and $N_{12} = -1$. We have then

$$A^{JM,-} = ((2J + 1)/4\pi)^{1/2} \int d\Omega e^{-iM\phi} d^J_{M0}(\theta) A(\theta,\phi)$$

and

$$A^{JM,+} = 0 \ , \qquad (46)$$

and the parity of these amplitudes is $P = -(-1)^J$.

The amplitude $A(\theta,\phi)$, given by eq. (11), may be written as

$$A(\theta,\phi) = A^{(1)}(\theta) + A^{(2)}(\theta).\cos\phi \qquad (47)$$

where

$$A^{(1)}(\theta) = ig_{a12}\left[sg^{s}(t_2)/(s_1 - m_a^2) + a_2 g^{t}(t_2)/(t_1 - m_2^2) + \right.$$

$$\left. + a_3 g^{u}(t_2)/(u_1 - m_1^2)\right] \qquad (48)$$

$$A^{(2)}(\theta) = ig_{a12} b\left[g^{t}(t_2)/(t_1 - m_2^2) - g^{u}(t_2)/(u_1 - m_1^2)\right] \qquad (49)$$

At HEA we have

$$a_2 \simeq s(E_2 + |\vec{p}_1|\cos\alpha\cos\theta)\sqrt{s_1}$$

$$a_3 \simeq s(E_1 - |\vec{p}_1|\cos\alpha\cos\theta)/\sqrt{s_1}$$

and

$$b \simeq s|\vec{p}_1|\operatorname{sen}\alpha\operatorname{sen}\theta/\sqrt{s_1} \qquad (50)$$

The integration on ϕ shows that there are non vanishing amplitudes only for $M = 0$ and $M = \pm 1$, and that

$$A^{J,M=-1,-} = - A^{J,M=+1,-}$$

We introduce the notation

$$A(L_J^P)_M = A^{J,M,-} \qquad (51)$$

where $J = L$, and the S, P and D partial wave amplitudes are given by

$$A(S_0^-)_0 = \pi^{1/2}\int_{-1}^{1} d(\cos\theta)\, d^0_{00}(\theta)A^{(1)}(\theta)$$

$$A(P_1^+)_0 = (3\pi)^{1/2}\int_{-1}^{1} d(\cos\theta)\, d^1_{00}(\theta)A^{(1)}(\theta)$$

$$A(P_1^+)_1 = ((3\pi)^{1/2}/2)\int_{-1}^{1} d(\cos\theta)\, d^1_{10}(\theta)A^{(2)}(\theta)$$

$$A(D_2^-)_0 = (5\pi)^{1/2}\int_{-1}^{1} d(\cos\theta)\, d^2_{00}(\theta)A^{(1)}(\theta)$$

$$A(D_2^-)_1 = ((5\pi)^{1/2}/2)\int_{-1}^{1} d(\cos\theta)\, d^2_{10}(\theta)A^{(2)}(\theta) \qquad (52)$$

For reactions of type $B(0^- \to 1^-, 0^-)$, the helicity amplitudes (23) and (24) have the form (B - 1).

$$A_{\lambda_1}(\theta,\phi) = e^{-i\lambda_1\phi}\tilde{A}_{\lambda_1}(\theta,\phi)\ , \qquad (53)$$

and the partial wave amplitudes are given by eqs. (B - 2) and (B - 5), for $\lambda_a = \lambda_2 = 0$ and $N_{12} = -1$:

$$A^{JM,\pm}_{\lambda_1} = ((2J+1)/8\pi)^{1/2}\int d\Omega e^{-iM\phi}\left\{ d^J_{M\lambda_1}(\theta)\tilde{A}_{\lambda_1}(\theta,\phi) \mp d^J_{M,-\lambda_1}(\theta)\tilde{A}_{-\lambda_1}(\theta,\phi)\right\} \qquad (54)$$

for $\lambda_1 = \pm 1$,

$$A^{JM,-}_{\lambda_1=0} = ((2J+1)/4\pi)^{1/2}\int d\Omega e^{-iM\phi} d^J_{Mo}(\theta)\tilde{A}_o(\theta,\phi) \qquad (55)$$

and $A^{JM,+}_{\lambda_1=0} = 0$ for $\lambda_1 = 0$.

The parities of these amplitudes are given by

$$P = \pm\,(-1)^J$$

From eqs. (23) and (24) we see that the expressions of $\tilde{A}_{\lambda_1}(\theta,\phi)$ have the form

$$\tilde{A}_{\lambda_1}(\theta,\phi) = A^{(1)}_{\lambda_1}(\theta) + A^{(2)}_{\lambda_1}(\theta)\cos\phi + A^{(3)}_{\lambda_1}(\theta)\sin\phi \qquad (56)$$

where, for $\lambda_1 = 0$ $A^{(3)}_{o}(\theta) = 0$, and for $\lambda_1 = \pm 1$; $A^{(1)}_{-1}(\theta) = -A^{(1)}_{1}(\theta)$ and $A^{(2)}_{-1}(\theta) = -A^{(2)}_{1}(\theta)$. The coefficients $A^{(i)}_{\lambda_1}(\theta)(i = 1,2,3)$ may be obtained from eqs. (23) and (24).

The integrations on ϕ in eqs. (54) and (55) show that only the values M = 0 and M = ± 1 correspond to non vanishing amplitudes.

As we are seeking for possible interferences among the components of TCDM we choose M = 0, which select the coefficients $A^{(1)}_{\lambda_1}(\theta)$. The coefficient $A^{(1)}_{o}(\theta)$ is the only one that contains the three components of TCDM, and is the more probable to gives rise to strong interferences.

From eqs. (54) and (55) we obtain, for M = 0:

$$A^{J,M=0,-}_{\lambda_1=0} = (\pi(2J+1))^{1/2}\int_{-1}^{1} d(\cos\theta)\, d^{J}_{oo}(\theta)A^{(1)}_{o}(\theta) \qquad (58)$$

$$A^{J,M=0,-}_{\lambda_1=1} = (2\pi(2J+1))^{1/2}\int_{-1}^{1} d(\cos\theta)\, d^{J}_{o1}(\theta)A^{(1)}_{1}(\theta)\ , \qquad (59)$$

$$A^{J,M=0,-}_{\lambda_1=-1} = A^{J,M=0,-}_{\lambda_1=1} \quad \text{and} \quad A^{J,M=0,+}_{\lambda_1} = 0.$$

The amplitudes for well defined orbital angular momentum are given by eq. (B - 10). Using the notation

$$A(L_J^P) = A_{(L)}^{J,M=0} \tag{60}$$

the S, P and D partial wave amplitudes are, for M = 0:

$$A(S_1^+) = (1/3)^{1/2}(2A_{\lambda_1=1}^{J=1,M=0,-} + A_{\lambda_1=0}^{J=1,M=0,-})$$

$$A(P_o^-) = - A_{\lambda_1=0}^{J=0,M=0,-}$$

$$A(P_2^-) = (2/5)^{1/2}(\sqrt{3}\, A_{\lambda_1=1}^{J=2,M=0,-} + A_{\lambda_1=0}^{J=2,M=0,-})$$

$$A(D_1^+) = (2/3)^{1/2}(A_{\lambda_1=1}^{J=1,M=0,-} - A_{\lambda_1=0}^{J=1,M=0,-})$$

$$A(D_3^+) = (1/7)^{1/2}(2\sqrt{2}\, A_{\lambda_1=1}^{J=3,M=0,-} + \sqrt{3}\, A_{\lambda_1=0}^{J=3,M=0,-}) \tag{61}$$

The helicity amplitudes for reactions of type C also factorize similarly to eq. (B - 1). The partial wave amplitudes are given by eq. (B - 2), for $\lambda_2 = 0$ and $N_{12} = -1$:

$$A_{\lambda_1\lambda_a}^{JM,\pm} = ((2J+1)/8\pi)^{1/2}\int d\Omega e^{-i(M-\lambda_a)\phi}\left\{d^J_{M\lambda_1}(\theta)\tilde{A}_{\lambda_1\lambda_a}(\theta,\phi) \mp d^J_{M,-\lambda_1}(\theta)\tilde{A}_{-\lambda_1,\lambda_a}(\theta,\phi)\right\} \tag{62}$$

and the parities of these amplitudes are

$$P = \pm\,(-1)^{J-1/2} \tag{63}$$

From the helicity amplitudes shown in eqs. (31) and (32) we see that

$$\tilde{A}_{\lambda_1\lambda_a}(\theta,\phi) = A^{(1)}_{\lambda_1\lambda_a}(\theta) + A^{(2)}_{\lambda_1\lambda_a}(\theta).\cos\phi + A^{(3)}_{\lambda_1\lambda_a}(\theta)e^{\mp i2\lambda_a\phi} \tag{64}$$

where the coefficients $A^{(i)}_{\lambda_1\lambda_a}(\theta)$ may be obtained from those amplitudes.

The integration on ϕ shows that the non vanishing amplitudes correspond to $M = \pm\lambda_a$ and $M = \lambda_a \pm 1$. We choose $M = \lambda_a$ because this condition selects the coefficients $A^{(I)}_{\lambda_1\lambda_a}(\theta)$. Only these coefficients contain the three components of TCDM, and are the most probable source of the interferences we are seeking for. From eqs. (62) and (64) we obtain for $M = \lambda_a$:

$$A^{J,M=\lambda_a,\pm}_{\lambda_1\lambda_a} = (\pi(J+1/2))^{1/2}\int_{-1}^{1} d(\cos\theta)\left[d^J_{\lambda_a\lambda_1}(\theta)A^{(1)}_{\lambda_1\lambda_a} \mp d^J_{\lambda_a,-\lambda_1}(\theta)A^{(1)}_{-\lambda_1,\lambda_a}(\theta)\right] \tag{65}$$

The partial wave amplitudes for well defined orbital angular momentum (L), according to eq. (B - 10), are

$$A^{J,M=\lambda_a,-}_{(L=J\mp1/2)\lambda_a} = 2(2J/(2J+1))^{1/2}\, C^{J-1/2,1/2,J}_{0,1/2,1/2}\, A^{J,M=\lambda_a,-}_{1/2,\lambda_a},$$

$$A^{J,M=\lambda_a,+}_{(L=J+1/2)\lambda_a} = 2(2(J+1)/(2J+1))^{1/2}\, C^{J+1/2,1/2,J}_{0,1/2,1/2}\, A^{J,M=\lambda_a,+}_{1/2,\lambda_a}$$

$$A^{J,M=\lambda_a,+}_{(L=J-1/2)\lambda_a} = 0 \quad \text{and} \quad A^{J,M=\lambda_a,-}_{(L=J+1/2)\lambda_a} = 0, \tag{66}$$

and satisfy the relations

$$A^{J,-1/2,\pm}_{(L=J\pm1/2),-1/2} = \pm A^{J,1/2,\pm}_{(L=J\pm1/2),1/2} \tag{67}$$

Introducing the notation

$$A(L_J^P)_{1/2} \equiv A^{J,M=1/2,\pm}_{(L)\,1/2} \tag{68}$$

the S, P and D waves are, for $M = \lambda_a = 1/2$,

$$A(S^-_{1/2})_{1/2} = \sqrt{2}\; A^{J=1/2,M=1/2,-}_{\lambda_1=1/2,\lambda_a=1/2}$$

$$A(P^+_{1/2})_{1/2} = -\sqrt{2}\; A^{J=1/2,M=1/2,+}_{\lambda_1=1/2,\lambda_a=1/2}$$

$$A(P^+_{3/2})_{1/2} = \sqrt{2}\; A^{J=3/2,M=1/2,-}_{\lambda_1=1/2,\lambda_a=1/2}$$

$$A(D^-_{3/2})_{1/2} = -\sqrt{2}\; A^{J=3/2,M=1/2,+}_{\lambda_1=1/2,\lambda_a=1/2}$$

$$A(D^-_{5/2})_{1/2} = \sqrt{2}\; A^{J=5/2,M=1/2,-}_{\lambda=1/2,\lambda_a=1/2}\ . \tag{69}$$

The partial wave amplitudes for reactions of type $D,(1/2^+ \to 3/2^+, 0^-)$, are given by eq. (B - 2) for $\lambda_2 = 0$ and $N_{12} = +1$, and the parities of these amplitudes are

$$P = \pm\,(-1)^{J-1/2} \tag{70}$$

The helicity amplitudes (41,42,43 and 44) factorize as eq. (B - 1) and the expressions for $\tilde{A}_{\lambda_1\lambda_a}(\theta,\phi)$ may be written in the form

$$\tilde{A}_{\lambda_1\lambda_a}(\theta) = A^{(1)}_{\lambda_1\lambda_a}(\theta) + A^{(2)}_{\lambda_1\lambda_a}(\theta).\cos\phi + A^{(3)}_{\lambda_1\lambda_a}(\theta).\sin\phi \tag{71}$$

As may be verified in the helicity amplitudes, only

the coefficients

$$A^{(1)}_{\pm 1/2,\pm 1/2}\ ,\ A^{(1)}_{\mp 1/2,\pm 1/2}\ ,\ A^{(2)}_{\pm 1/2,\pm 1/2}\ \text{ and }\ A^{(2)}_{\mp 1/2,\pm,1/2}$$

contain the three components of TCDM, consequently if there exists strong interferences of TCDM type they are expected to occur in these coefficients. The other coefficients contain only one or two of the TCDM components.

The integration on ϕ that appears in eq. (B - 2) may be performed using eq. (71), and shows that the non vanishing amplitudes correspond to $M = \lambda_a$ and $M = \lambda_a \pm 1$.

As we want to show that there may happen interferences in the partial wave amplitudes, we choose, as simplifying, only $M = \lambda_a$. This choice selects the coefficients $A^{(1)}_{\lambda_1\lambda_a}(\theta)$ in which the strong interferences are expected to occur.

The partial wave amplitudes for $M = \lambda_a$ are

$$A^{J,M=\lambda_a,\pm}_{\lambda_1\lambda_a} = (\pi(J+1/2))^{1/2}\int_{-1}^{1} d(\cos\theta)\left[d^J_{\lambda_a\lambda_1}(\theta)A^{(1)}_{\lambda_1\lambda_a}(\theta) \pm d^J_{\lambda_a,-\lambda_1}(\theta)A^{(1)}_{-\lambda_1,\lambda_a}(\theta)\right] \tag{72}$$

and the partial wave amplitudes for well defined orbital angular momentum (L), given by eq. (B - 10), for $M = \lambda_a$ read

$$A^{J,M=\lambda_a,+}_{(L=J-3/2)\lambda_a} = A^{J,M=\lambda_a,+}_{(L=J-1/2)\lambda_a} = A^{J,M=\lambda_a,-}_{(L=J+1/2)\lambda_a} = A^{J,M=\lambda_a,+}_{(L=J+3/2)\lambda_a} = 0 \tag{73}$$

and

$$A^{J,M=\lambda_a,+}_{(L=J-3/2)\lambda_a} = \left\{((2J+3)/J)^{1/2}\, A^{J,M=\lambda_a,+}_{3/2,\lambda_a} + (3(2J-1)/J)^{1/2}\, A^{J,M=\lambda_a,+}_{1/2,\lambda_a}\right\}/2$$

$$A^{J,M=\lambda_a,-}_{(L=J-1/2)\lambda_a} = -\left\{(3(2J+3)/(J+1))^{1/2} A^{J,M=\lambda_a,-}_{3/2,\lambda_a} + ((2J-1)/(J+1))^{1/2}\, A^{J,M=\lambda_a,-}_{1/2,\lambda_a}\right\}/2$$

$$A^{J,M=\lambda_a,+}_{(L=J+1/2)\lambda_a} = \left\{(3(2J-1)/J)^{1/2}\, A^{J,M=\lambda_a,+}_{3/2,\lambda_a} - ((2J+3)/J)^{1/2}\, A^{J,M=\lambda_a,+}_{1/2,\lambda_a}\right\}/2$$

$$A^{J,M=\lambda_a,-}_{(L=J+3/2)\lambda_a} = \left\{((2J-1)/(J+1))^{1/2}\, A^{J,M=\lambda_a,-}_{3/2,\lambda_a} + (3(2J+3)/(J+1))^{1/2}\, A^{J,M=\lambda_a,-}_{1/2,\lambda_a}\right\}/2 \qquad (74)$$

These amplitudes satisfy the relations

$$A^{J,-\lambda_a,\pm}_{(L),-\lambda_a} = \pm\, A^{J,\lambda_a,\pm}_{(L),\lambda_a} \qquad (75)$$

To denote these amplitudes we define

$$A(L^P_J)_{1/2} = A^{J,M=1/2,\pm}_{(L)\lambda_a=1/2} \qquad (76)$$

Using (74) with the notation (76), the S, P and D partial wave amplitudes read:

$$A(S^-_{3/2})_{1/2} = A^{3/2,1/2,+}_{3/2,1/2} + A^{3/2,1/2,+}_{1/2,1/2,}$$

$$A(P^+_{1/2})_{1/2} = -\sqrt{2}\, A^{1/2,1/2}_{1/2,1/2}$$

$$A(P^+_{3/2})_{1/2} = -(1/5)^{1/2}(3\, A^{3/2,1/2,-}_{3/2,1/2} + A^{3/2,1/2,-}_{1/2,1/2})$$

$$A(P^+_{5/2})_{1/2} = (1/5)^{1/2}(2\, A^{5/2,1/2,+}_{3/2/,1/2} + \sqrt{6}\, A^{5/2,1/2,+}_{1/2,1/2})$$

$$A(D^-_{1/2})_{1/2} = \sqrt{2}\, A^{1/2,1/2,-}_{1/2,1/2}$$

$$A(D^-_{3/2})_{1/2} = A^{3/2,1/2,+}_{3/2,1/2} - A^{3/2,1/2,+}_{1/2,1/2}$$

$$A(D^-_{5/2})_{1/2} = -(2/7)^{1/2}\,(\sqrt{6}\, A^{5/2,1/2,-}_{3/2,1/2} + A^{5/2,1/2-}_{1/2,1/2})$$

$$A(D^-_{7/2})_{1/2} = (1/7)^{1/2}(\sqrt{5}\, A^{7/2,1/2,+}_{3/2,1/2} + 3\, A^{7/2,1/2,+}_{1/2,1/2}) \qquad (77)$$

RESULTS AND CONCLUSIONS

In this paper we analyse the TCDM applications to several types of (DDR). A part of the results presented here was not published previously. We put together all spin-parity structures of the subreaction a + IP → 1 +2. These amplitudes can be useful for a complete understanding to the (DDR) phenomenology. In this sense the model is universal, describing the multiple aspects of the data. The TCDM is a natural consequence of the earlier Diell-Hiida-Deck- Model[6] until the discovery of the slope (B), mass (M_{12}), angular ($\cos\theta^{G.J.}$) and the slope-mass-partial waves correlations[7].

The application of TCDM to these different types of reactions permits us testing the model in those reactions for which there are experimental results, and to give a theoretical prediction for the others.

The DDR studied here have different spin and parity structures in the subreactions (a + IP → 1 + 2).

The reactions studied here have the following spin and parity structures in the dissociative process $(a \to 1 + 2)$, $(J_a^{P_a} \to J_1^{P_1} + J_2^{P_2})$: A-$(0^- \to 0^+, 0^-)$, B-$(0^- \to 1^-, 0^-)$, C-$(1/2^+ \to 1/2^+, 0^-)$ and D-$(1/2^+ \to 3/2^+, 0^-)$.

We choose only one reaction of each type to apply the TCDM. The reactions chosen are respectively:
A-: $K + p \to (k + \pi) + p$, B-: $K + p \to (K^* + \pi) + p$, C-: $p + p \to (n + \pi^-) + p$, and D-: $p + p \to (\Delta^{++} + \pi^-) + p$.

Following we discuss the results obtained for each reaction.

The reactions of type A have the simplest spin and parity structure. The TCDM for these reactions may be reggeized, what extends the validity of the model beyond the region of resonances in the dissociated subsystem (1 + 2).

The partial wave amplitudes for the reaction $K + p \to (k + \pi) + p$ are given by eq. (52). A slope-mass correlation may be observed in S wave. The fig. (4) shows the theoretical distributions for the S wave in the effective mass ranges $1.25 \leq M_{k\pi} \leq 1.35$GeV and $1.35 \leq M_{k\pi} \leq 1.50$GeV respectively.

The slopes of these distributions, calculated in the interval $0 \leq |t_2| \leq 0.002$ GeV^2, are repectively $B = 14.6\,\text{GeV}^{-2}$ and $B = 11.8\,\text{GeV}^{-2}$. These results may be compared with the experimental ones[8], showed in fig. (8).

The parameters of TCDM used to obtain the results above are: $\sigma_{tot}^{\pi N} = 23$ mb, $\sigma_{tot}^{KN} = 20$ mb, $\sigma_{tot}^{kN} = 24$ mb, $B_{\pi N} = 7\,\text{GeV}^{-2}$, $B_{KN} = 6.5\,\text{GeV}^{-2}$ and $B_{kN} = 6.5\,\text{GeV}^{-2}$.

The reaction of type B studied here is $K + p \to (K^* + \pi) + p$. The helicity amplitudes and the partial wave amplitudes are

given by eqs. (23) and (61) respectively.

A slope mass correlation may be observed in the S and P waves. In figs. (5,6,7) we see the distributions for 1^+S and 0^-P waves, restricted by M = 0, in the effective mass ranges $1.04 \leq M_{K^*\pi} \leq 1.20\,GeV$, $1.20 \leq M_{K^*\pi} \leq 1.35\,GeV$ and $1.35 \leq M_{K^*\pi} \leq 1.50\,GeV$.

The slopes of these distributions calculated in the interval $0 \leq |t_2| \leq 0.02\,GeV^2$, are given in those figures.

The results for the two higher mass intervals may be compared with the experimental distributions[8] and slopes of fig. (8).

The TCDM parameters used to find these experimental slopes are $\sigma_{tot}^{\pi N} = 22$ mb, $\sigma_{tot}^{K^*N} = 18$ mb, $\sigma_{tot}^{KN} = 21$ mb, $B_{\pi N} = 9.0\,GeV^{-2}$, $B_{K^*N} = 4.5\,GeV^{-2}$ and $B_{KN} = 3.0\,GeV^{-2}$.

As may be observed in fig. 5 there exists a strong interference in the 0^-P wave, whose slope is much higher than that of the 1^+S wave. As a consequence of that interference there appears a dip in the 0^-P wave. The dip deslocates slowly to higher values of $|t_2|$ as $M_{K^*\pi}$ increases.

It must be remembered however that in the mass intervals where the data are given, mainly in the higher ones, there exists $K^*\pi$ resonances.

The dip in the 0^-P wave, predicted by the model, is not seen in the data. Possibly it is covered by resonance effects, or the large errors near $t_2 = -0.3\,GeV^2$ do not permits distinghish it.

The reaction of type C, $p + p \to (n + \pi^+) + p$, permits an excellent test for the TCDM. This reaction has the best data among the DDR. A clear slope-mass-$\cos\theta^{GJ}$ correlation may be

observed in these data.

That reaction has some spin complications. However the TCDM may be reggeized and dualized. Two parametrizations have been obtained for the dualized TCDM. The dual resonance parametrization (DRP) is obtained according the Veneziano ansatz. We cannot expect that the theoretical mass spectrum fits well the experimental one with this rigid parametrization.

To obtain a parametrization more flexible to describe the resonances, it may be used the dual reggeized Deck parametrization. In this case the Veneziano functions are replaced by their Regge limits.

The fits of these parametrizations to the data are show in figs. (9) to (16). The values of the (TCDM) parameters (which are the same for the two cases) are: $\sigma_{tot}^{\pi p} = 25$ mb, $\sigma_{tot}^{np} = 30$ mb, $\sigma_{tot}^{pp} = 40$ mb, $B_{\pi p} = 10\,GeV^{-2}$, $B_{np} = B_{pp} = 9\,GeV^{-2}$ and $\lambda = 0.3\,GeV$.

The total mass spectrum, fig. (9), fixes the overall normalizations for the two parametrizations. Fig. (10) shows the $d\sigma/dt_2$ distributions for some windows in $M_{n\pi}$ and $\cos\theta^{GJ}$. These windows appear in fig. (11), where the zeros of the amplitudes, determined by the eqs. (29), are located. Fig. (12) shows the net diffractive slope (B) as a function of the effective mass and the good fitting of the slope predicted by the DRP.

There is a satisfactory agreement of the parametrizations with the $\cos\theta^{GJ}$ and ϕ^{GJ} distributions, fig. (13). The (TCDM) dualized reproduces well the turnover of the $\cos\theta^{GJ}$ dsitribution at $\cos\theta^{GJ} = +1$.

Although there are no experimental results to be confronted with, it is interesting to see how the slope mass correlation appears in partial waves. Figs. (14,15,16) show the S, P and D wave distributions, restricted by $M = \lambda_a$. It may be seen that the strongest interferences occur in the P and D waves, in which there appear dips and turnovers.

Another reaction, of the same type, which is very well described by the dualized TCDM is $p + p \to (\Lambda + K^+) + p$. See figures (17-21) taken from reference [1c]. Where the comparison with the experimental data was made.

The reaction of type D analyzed here, $p + p \to (\Delta^{++} + \pi^-) + p$, has helicity amplitudes and partial wave amplitudes given by eqs. (41-44) and (77) respectively. The complexity of these amplitudes does not permit derive simple equations to determine the positions of possible zeros. But the numerical calculations of $d\sigma/dt_2$ show that there exists slope-mass correlations in the distributions for that reaction. In fig. (22) we see that the slope decreases as the effective mass increases. Fig. (23) shows as the slope depends on the effective mass and on the $\cos\theta^{GJ}$ intervals.

The set of parameters of TCDM used in this calculations are $\sigma_{tot}^{\pi N} = 25$ mb, $\sigma_{tot}^{NN} = 40$ mb, $\sigma_{tot}^{N\Delta} = 50$ mb, $B_{\pi N} = 10\,GeV^{-2}$, $B_{NN} = 9\,GeV^{-2}$ and $B_{N\Delta} = 8\,GeV^{-2}$, and the slopes are calculated in the interval $0 \leq |t_2| \leq 0.02\,GeV^2$.

The best way to see the slope mass correlation in this reaction is to look at the partial wave distributions. It must be remembered that the partial wave distributions here are restricted by the condition $M = \lambda_a$. This condition has the ad-

vantage of simplifying the calculations and is enough to verify a possible slope-mass-partial wave correlation.

In fig. (24) we see the S, P and D wave distributions for two effective mass intervals. The S wave shows a strong interference, with a dip at $t_2 \simeq -0.35\,GeV^2$.

The examination of each amplitude $A(L^P_J)_{1/2}$, for P and D wave distributions, allows us to seek for interference structures not seen in fig. (24).

Fig. (25) shows the $A(P^+_{1/2})_{1/2}$, $A(P^+_{3/2})_{1/2}$ and $A(P^+_{5/2})_{1/2}$ distributions. Among these, the $A(P^+_{3/2})_{1/2}$ is the one that shows the strongest interference, with a dip at $t_2 \simeq -0.1\,GeV^2$.

The relative normalization in fig. (25) shows that the partial wave $A(P^+_{1/2})_{1/2}$ is two orders of magnitude higher than $A(P^+_{3/2})_{1/2}$, where the strongest interference occurs. By this reason the total P wave distributions, showed in fig.(24), do not present dips.

The D wave spectrum for each J, i.e, $A(D^-_{1/2})_{1/2}$, $A(D^-_{3/2})_{1/2}$, $A(D^-_{5/2})_{1/2}$ and $A(D^-_{7/2})_{1/2}$ wave distributions are showed in fig. (26). We remark that only the $A(D^-_{1/2})_{1/2}$ and $A(D^-_{7/2})_{1/2}$ waves present dips at $t_2 \simeq -0.6\,GeV^2$ and $t_2 \simeq -0.4\,GeV^2$ respectively. The total D wave distribution, showed in fig. (24) do not present dips because all the contributions from different values of J are added.

The net slopes for each wave, calculated in the interval $0 \leq |t_2| \leq 0.02\,GeV^2$, are shown in tables D - 1 and D - 2 At table D - 2 we remark that all the waves, but $P_J = 3/2$, present an expected mass-slope-partial wave correlation, that

is, the slope decreases as the effective mass $M_{\Delta\pi}$ increases.

The abnormal behaviour of the $P_{J=3/2}$ is because the zero occurs for smaller $|t_2|$ when s_1 increases.

APPENDIX A

This appendix contains a summary of the kinematical variables and expressions used in this paper.

The DDR a + b → (1 + 2) + 3 may be represented as in fig. (1), and the TCDM which describes these reactions has the diagrams of fig. (2).

The fourmomenta corresponding to the external lines are p_i (i = a,b,1,2,3) and for the internal lines we define.

$$q = p_a - p_1,\ k = p_a - p_2 \text{ and } p = p_1 + p_2 \ . \qquad \text{(A-1)}$$

At the diffractive vertices the following fourmomenta are used:

$$P = (p_1+k)/2 \ , \ Q = (p_2 + q)/2,$$

$$K = (p_a+p)/2 \ , \ R = (p_b + p_3)/2 \ . \qquad \text{(A-2)}$$

The invariants constructed with these 4-vectors are,

$$s = (p_a + p_b)^2,\ s_1 = (p_1 + p_2)^2,\ s_2 = (p_2 + p_3)^2,$$

$$s_3 = (p_1 + p_3)^2,\ t_1 = (p_a - p_1)^2,\ u_1 = (p_a - p_2)^2,$$

$$t_2 = (p_b - p_3)^2 \qquad \text{(A-3)}$$

The energies E_i and the momenta $|\vec{p}_i|$ $(i = a,b,1,2,3)$ are defined in the Gottfried-Jackson frame for $(\vec{p}_1 + \vec{p}_2 = 0)$ $(1+2)$ rest system (see fig. 27). The expressions of E_i and $|\vec{p}_i|$ are given by,

$$E_a = (s_1 + m_a^2 - t_2)/2\sqrt{s_1} \ , \ E_b = (s_1 - m_a^2 - m_3^2 + t_2)/2\sqrt{s_1} \ ,$$

$$E_1 = (s_1 + m_1^2 - m_2^2)/2\sqrt{s_1} \ ; \ E_2 = (s_1 + m_2^2 - m_1^2)/2\sqrt{s_1} \ ,$$

$$E_3 = (s - s_1 - m_3^2)/2\sqrt{s_1} \ , \ |\vec{p}_a| = \lambda^{1/2}(s_1, m_a^2, t_2)/2\sqrt{s_1} \ ,$$

$$|\vec{p}_b| = \lambda^{1/2}(s_1, m_b^2, t_{a3})/2\sqrt{s_1} \ , \ |\vec{p}_3| = \lambda^{1/2}(s_1, m_3^2, s)/2\sqrt{s_1}$$

$$\text{and } |\vec{p}_1| = |\vec{p}_2| = \lambda^{1/2}(s_1, m_1^2, m_2^2)/2\sqrt{s_1} \ , \qquad \text{(A-4)}$$

where

$$t_{a3} = s_1 - s - t_2 + m_a^2 + m_b^2 + m_3^2$$

and $\lambda(x,y,z)$ is defined by

$$\lambda(x,y,z) = x^2 + y^2 + z^2 - 2(xy + xz + yz) \qquad \text{(A-5)}$$

The angular coordinates of the momenta are:

$$\vec{p}_1 = \vec{p}_1(\theta,\phi), \ \vec{p}_b = \vec{p}_b(\chi,0) \quad \text{and} \quad \vec{p}_3 = \vec{p}_3(\alpha,0), \qquad \text{(A-7)}$$

The angles in GJS are related by

$$\cos\beta = \cos\alpha \cos\theta + \operatorname{sen}\alpha \operatorname{sen}\theta \cos\phi. \qquad \text{(A-8)}$$

High energy approximations (HEA)

These approximations correspond to

$$s, s_2, s_3 >> s_1, |t_1|, |u_1|, |t_2|, m_i^2 \quad (i = a,b,1,2,3). \tag{A-9}$$

Using (A-9) we obtain

$$2Q.R \simeq s_2, \quad 2P.R \simeq s_3 \text{ and } 2K.R \simeq s \quad , \tag{A-10}$$

$$\cos\alpha \simeq -(s_1 - m_a^2 + t_2)/\lambda^{1/2}(s_1, m_a^2, t_2) \text{ and}$$

$$\text{sen}\,\alpha \simeq 2\sqrt{s_1}\sqrt{-t_2}/\lambda^{1/2}(s_1, m_a^2, t_2) \quad , \tag{A-11}$$

$$s_2 \simeq s(E_2 + |\vec{p}_1|\cos\beta)/\sqrt{s_1} \text{ and } s_3 \simeq s(E_1 - |\vec{p}_1|\cos\beta)/\sqrt{s_1} \tag{A-12}$$

For very small values of $|t_2|$ the relation (A-8) becomes

$$\cos\beta \simeq -\cos\theta + (2\sqrt{s_1}\sqrt{-t_2}/(s_1 - m_a^2))\text{sen}\,\theta\cos\phi \quad , \tag{A-13}$$

then, carrying into (A-12) we obtain

$$s_2 \simeq s(E_2 - |\vec{p}_1|\cos\theta)/\sqrt{s_1} + (2s|\vec{p}_1|\sqrt{-t_2}/(s_1 - m_a^2))\text{sen}\,\theta\cos\phi$$

and

$$s_3 \simeq s(E_1 + |\vec{p}_1|\cos\theta)/\sqrt{s_1} - (2s|\vec{p}_1|\sqrt{-t_2}/(s_1 - m_a^2))\text{sen}\,\theta\cos\phi \tag{A-14}$$

At the same approximations we have

$$(t_1 - m_2^2) \simeq -(s_1 - m_a^2)(E_2 - |\vec{p}_1|\cos\theta)/\sqrt{s_1} \quad \text{and}$$

$$(u_1 - m_1^2) \simeq -(s_1 - m_a^2)(E_1 + |\vec{p}_1|\cos\theta)/\sqrt{s_1} \tag{A-15}$$

From (A-14) and (A-15) we obtain

$$\frac{s_3}{u_1 - m_1^2} \simeq -\frac{s}{s_1 - m_a^2}\left[1 - \frac{2|\vec{p}_1|\sqrt{s_1}\sqrt{-t_2}\,\text{sen}\,\theta\cos\phi}{(s_1 - m_a^2)(E_1 + |\vec{p}_1|\cos\theta)}\right]$$

and

$$\frac{s_2}{t_1 - m_2^2} \simeq -\frac{s}{s_1 - m_a^2}\left[1 + \frac{2|\vec{p}_1|\sqrt{s_1}\sqrt{-t_2}\,\text{sen}\,\theta\cos\phi}{(s_1 - m_a^2)(E_2 - |\vec{p}_1|\cos\theta}\right] \quad , \tag{A-16}$$

and at the limit $t_2 = 0$, we have the relation

$$\frac{s_2}{t_1 - m_2^2} \simeq \frac{s_3}{u_1 - m_1^2} \simeq -\frac{s}{s_1 - m_a^2} \quad . \tag{A-17}$$

For a three particles final state reaction the cross-section is given by

$$d\sigma = C\int \frac{\lambda^{1/2}(s_1, m_1^2, m_2^2)}{s_1} ds_1 dt_2 d\cos\theta\, d\phi\, |A|^2 \tag{A-18}$$

where

$$C = 1/(2^{10}\pi^4\lambda(s, m_a^2, m_b^2)).$$

APPENDIX B

Partial wave projection of the final state subsystem (1 +2) of a a + b → (1 + 2) + 3, (DDR).

In this appendix we collect some results usefull to the projection into partial waves of the helicity amplitudes, obtained through the TCDM, for the DDR.

Neglecting the spin structure of (bIP3) vertex, due to the factorization property, the helicity amplitude, given by the TCDM for the DDR a + b → (1 +2) +3, in the GJS, making use of the Jacob-Wick convention, has an explicit phase,

$$A_{\lambda_1\lambda_2\lambda_a}(s,s_1,t_2;\theta,\phi) = e^{-i(\lambda-\lambda_a)\phi}\,\tilde{A}_{\lambda_1\lambda_2\lambda_a}(s,s_1,t_2;\theta,\phi) \qquad (B\text{-}1)$$

where $\lambda = \lambda_1 - \lambda_2$.

The helicity amplitudes for total angular momentum (J), of the dissociated subsystem (1 + 2) and its projection (M), on the incident beam direction ($\vec{p}_a$), and normality (±), are given by

$$A^{JM\pm}_{\lambda_1\lambda_2\lambda_a}(s,s_1,t_2) = ((2J+1)/8\pi)^{1/2}\int d\Omega\; e^{-(M-\lambda_a)\phi}\; x$$

$$x\left\{d^J_{M\lambda}(\theta)\tilde{A}_{\lambda_1\lambda_2\lambda_a}(\theta,\phi) \pm N_{12}\, d^J_{M,-\lambda}(\theta)\tilde{A}_{-\lambda_1,-\lambda_2,\lambda_a}(\theta,\phi)\right\} \qquad (B\text{-}2)$$

where

$$N_{12} = \eta_1\eta_2(-1)^{\delta_1+\delta_2-v_{12}} \qquad (B\text{-}3)$$

In the above expression η_1 and η_2 and δ_1 and δ_2 are

the intrinsic parities and spins of the particles (1) and (2) respectively;, $v_{12} = 0$ for J integer and $v_{12} = 1/2$ for J half integer.

The parities of the amplitudes are given by

$$P = \pm(-1)^{J-v_{12}} \tag{B-4}$$

For $\lambda_1 = \lambda_2 = 0$ instead of (B - 2)we have

$$A^{JM,N}_{oo,\lambda_a 12} = ((2J+1)/4\pi)^{1/2}\int d\Omega\, e^{-i(M-\lambda_a)\phi} d^J_{M0}(\theta)\tilde{A}_{oo\lambda_a}(\theta,\phi). \tag{B-5}$$

From parity conservation we obtain the relation:

$$A^{J,-M,\pm}_{-\lambda_1,-\lambda_2,-\lambda_a} = \eta(-1)^{M\mp\lambda_a} A^{JM,\pm}_{\lambda_1\lambda_2\lambda_a} \tag{B-6}$$

where

$$\eta = \eta_1\eta_2\eta_a(-1)^{\delta 1+\delta 2-\delta a} \tag{B-7}$$

The amplitudes (B - 2) also satisfy the relation

$$A^{JM,\pm}_{-\lambda_1,-\lambda_2,\lambda_a} = \pm N_{12}\, A^{JM,\pm}_{\lambda_1\lambda_2\lambda_a} \tag{B-8}$$

The amplitudes for well defined J,M, orbital angular momentum L, spin $\vec{\delta} = \vec{\delta}_1 + \vec{\delta}_2$ and normality (±), of the subsystem (1 +2), are given by

$$A^{JM,\pm}_{(L,\delta)\lambda_a} = ((2L+1)/(2J+1))^{1/2} \sum_{\lambda_1\lambda_2} C^{L\delta J}_{o\lambda\lambda}\, C^{\delta_1\delta_2\delta}_{\lambda_1,-\lambda_2,\lambda}\, A^{JM,\pm}_{\lambda_1\lambda_2\lambda_a} \tag{B-9}$$

where $C^{L\delta J}_{o\lambda\lambda}$ and $C^{\delta_1\delta_2\delta}_{\lambda_1,-\lambda_2,\lambda}$ are the Clebsh-Gordan coeficients. In the cases for which $\delta_2 = 0$, $\delta = \delta_1$, the amplitudes (B-9) become

$$A^{JM,\pm}_{(L)\lambda_a} = ((2L+1)/(2J+1))^{1/2}\left[\bar{1} \pm N_{12}(-1)^{J-L-\delta_1}\right]\sum_{|\lambda_1|} C^{L\delta_1 J}_{o|\lambda_1||\lambda_1|} A^{JM,\pm}_{|\lambda_1|,\lambda_a} \qquad \text{(B-10)}$$

From the relations (B - 6) and (B - 8) we obtain

$$A^{J,-M,\pm}_{(L),-\lambda_a} = \pm N_{12}\cdot\eta(-1)^{M-\lambda_a} A^{J,M,\pm}_{(L)\lambda_a} \quad . \qquad \text{(B-11)}$$

TABLE D1 - Values of the slopes in GeV^{-2} corresponding to the curves $d\sigma/dt_2$ shown at Fig.(D - 3).

L	$1.37 \leq M_{\Delta\pi} \leq 1.40GeV$	$1.40 \leq M_{\Delta\pi} \leq 1.45GeV$
S	B = 19.5	B = 17.4
P	B = 9.7	B = 7.3
D	B = 16.7	B = 16.1

TABLE D2 - Values of the slopes in GeV^{-2} for each wave with (L) and (J) well defined, shown at figs.(D-4) and (D-5).

L	J	$1.37 \leq M_{\Delta\pi} \leq 1.40GeV$	$1.40 \leq M_{\Delta\pi} \leq 1.45GeV$
P	1/2	B = 7.1	B = 4.5
	3/2	B = 24.2	B = 33.2
	5/2	B = 22.8	B = 18.1
D	1/2	B = 17.2	B = 16.4
	3/2	B = 13.4	B = 13.0
	5/2	B = 18.9	B = 13.2
	7/2	B = 43.2	B = 34.7

FIGURE CAPTIONS

Fig. 1 - Single Pomeron exchange in the a + b → (1 + 3) + 2 reaction at high energy.

Fig. 2 - The three components of the (TCDM), representing the t_1-channel, u_1-channel and s_1-channel of the a + b → (1 + 2) + 3 reaction.

Fig. 3 - Graphical representation of the Pomeron factorization property.

Fig. 4 - Partial wave (0^-S) t_2-distributions and slopes of the reaction Kp → (kπ)p, for two effective mass ranges.

Fig. 5 - (1^+S) and (0^-P) partial wave distributions and slopes of the reaction Kp → (K*π)p, in the effective mass range $1.04 \leq M_{K^*\pi} \leq 1.20$ (GeV).

Fig. 6 - The same as fig. (5) for $1.20 \leq M_{K^*\pi} \leq 1.35$ (GeV)

Fig. 7 - The same as Fig. (5) for $1.35 \leq M_{K^*\pi} \leq 1.50$ (GeV)

Fig. 8 - Experimental results of the partial wave cross sections for the reactions Kp → (kπ)p - (0^-S) and Kp → (K*π)p - (1^+S and 0^-P), in two effective mass ranges[8].

Fig. 9 - Effective mass ($M_{N\pi}$) distributions of the reaction Np → (Nπ)p for (a) $-0.1 < t_2 < 0.02$; (b) $-0.08 < t_2 < -0.02$ and (c) $-1.0 < t_2 < -0.2$. The full line represents the dual Deck parametrization and the dotted line represents the dual resonance parametrization[1a].

Fig. 10 - t_2 distributions integrated in several regions of $M_{N\pi}$ and $\cos\theta^{GJ}$.

Fig. 11 - The location of the zero of the amplitude for $Np \to (N\pi)p$, as a function of $\cos\theta^{GJ}$, $M_{N\pi}$ and t_2. The rectangles labelled from (a) to (ℓ) are the regions in $\cos\theta^{GJ}$ and $M_{N\pi}$ in which the t_2 distributions of fig. (10) are integrated.

Fig. 12 - The t_2 slope as a function of $M_{N\pi}$.

Fig. 13 - (a) $\cos\theta^{GJ}$ distribution for $1.08 < M_{N\pi} < 1.4$ (GeV) and $-0.23 < t_2 < 0$. (b) ϕ^{GJ} distribution for $1.2 < M_{N\pi} < 1.375$ (GeV), $-0.2 < t_2 < -0.02$ and $0.8 < \cos\theta^{GJ} < 1$. (c) The same as (b) except $-1 < \cos\theta^{GJ} < -0.8$.

Fig. 14 - S, P and D partial wave t_2 distributions for the reaction $Np \to (N\pi)p$ integrated in two effective mass ranges, and restricted to ($M = \lambda_a$).

Fig. 15 - $P_{(J=1/2)}$ and $P_{(J=3/2)}$ partial wave t_2 distributions.

Fig. 16 - $D_{(J=3/2)}$ and $D_{(J=5/2)}$ partial wave t_2 distributions.

Fig. 17 - The mass distribution of the (ΛK^+) system. The full line shows the results of the (TCDDM)[1c].

Fig. 18 - $d\sigma/dt_2$ distributions for various $M(\Lambda K^+)$ intervals, integrated over all $\cos\theta^{GJ}$ and ϕ^{GJ}. (a) for all $M(\Lambda K)$ masses, (b) for $1.61 \leq M(\Lambda K) \leq 1.8$GeV, (c) for $1.8 \leq M(\Lambda K) \leq 2.0$GeV, (d) for $2.0 \leq M(\Lambda K) \leq 2.5$GeV.

Fig. 19 - $d\sigma/dt_2$ distributions for some $\cos\theta^{GJ}$ regions, for all masses of ΛK^+ system and integrated over all ϕ^{GJ} (a) in the interval $\cos\theta^{GJ} < -0.5$; (b) for $|\cos\theta^{GJ}| \leq 0.5$; (c) $\cos\theta^{GJ} \geq 0.8$ (full line), $\cos\theta^{GJ} \geq 0.5$ (dotted line).

Fig. 20 - Theoretical $d\sigma/dt_2$ distributions calculated by (TCDDM). (a) In the intervals $1.61 \leq M(\Lambda K) \leq 1.7$ (GeV) and $-0.5 \leq \cos\theta^{GJ} \leq -0.3$. (b) In the intervals

$1.7 \leq M(\Lambda K) \leq 1.8$ (GeV) and $-0.5 \leq \cos\theta^{GJ} \leq -0.3$.

Fig. 21 - Gottfried-Jackson angle distributions for all masses $M(\Lambda K)$ and for $0 \leq |t_2| \leq 1$. (a) $\cos\theta^{GJ}$ distribution integrated over all ϕ^{GJ}. (b) ϕ^{GJ} distribution integrated over all $\cos\theta^{GJ}$.

Fig. 22 - t_2 distributions and slopes, for reaction $pp \to (\Delta^{++}\pi^-)p$, integrated in two effective mass ranges.

Fig. 23 - t_2 distributions and slopes, for $pp \to (\Delta^{++}\pi^-)p$, integrated in two intervals of $M_{\Delta\pi}$ and three intervals of $\cos\theta^{GJ}$.

Fig. 24 - S, P and D partial wave t_2 distributions, restricted to $(M = \lambda_a)$.

Fig. 25 - $P_{(J=1/2)}$, $P_{(J=3/2)}$ and $P_{(J=5/2)}$ partial wave t_2 distributions, restricted to $(M = \lambda_a)$.

Fig. 26 - $D_{(J=1/2)}$, $D_{(J=3/2)}$, $D_{(J=5/2)}$ and $D_{(J=7/2)}$ partial wave t_2 distributions, restricted to $(M = \lambda_a)$.

Fig. 27 - Gottfried-Jackson coordinates for $R12(\vec{p}_1 + \vec{p}_2 = 0)$.

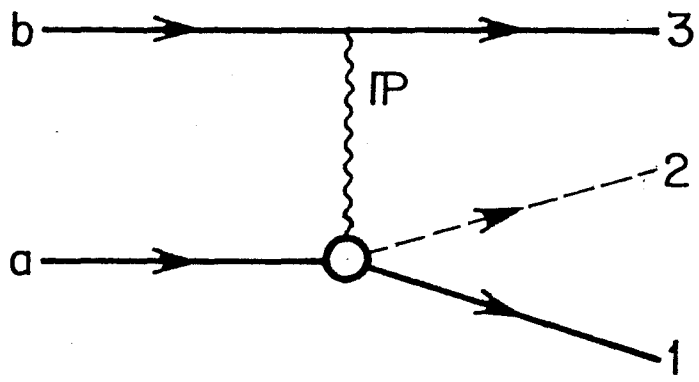

Fig. 1

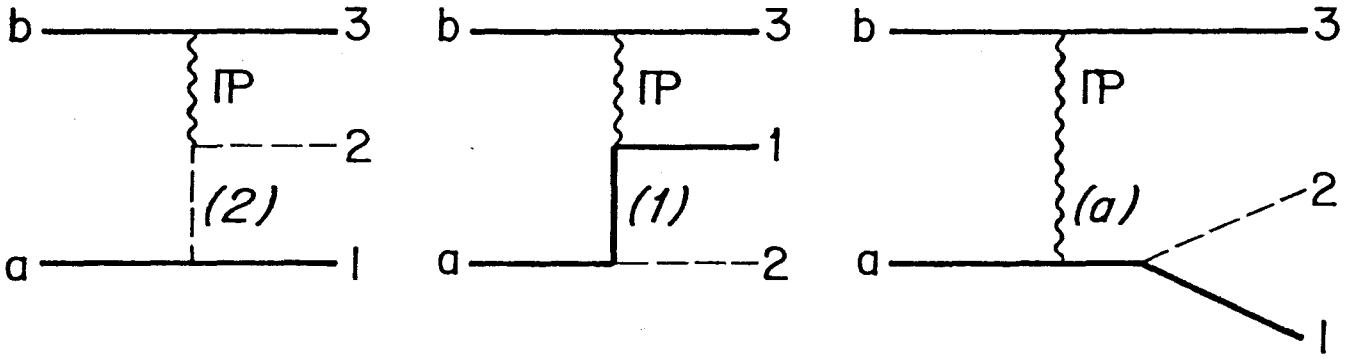

Fig. 2

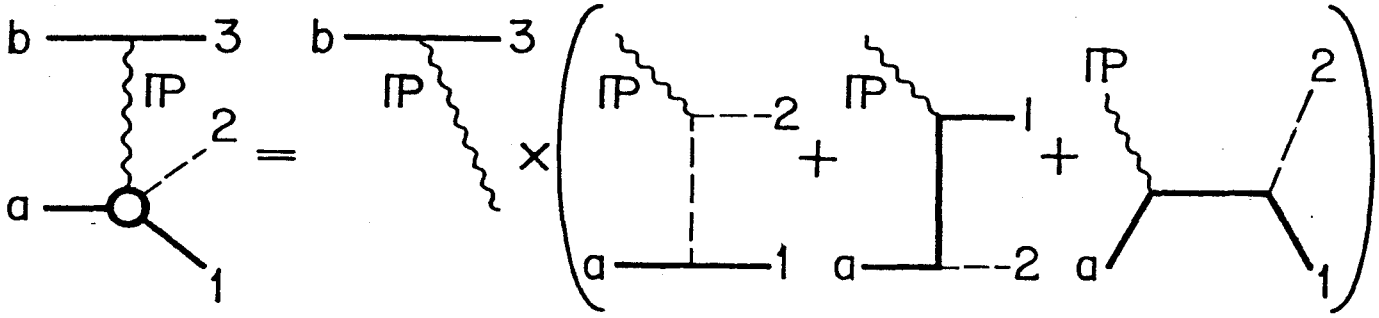

Fig. 3

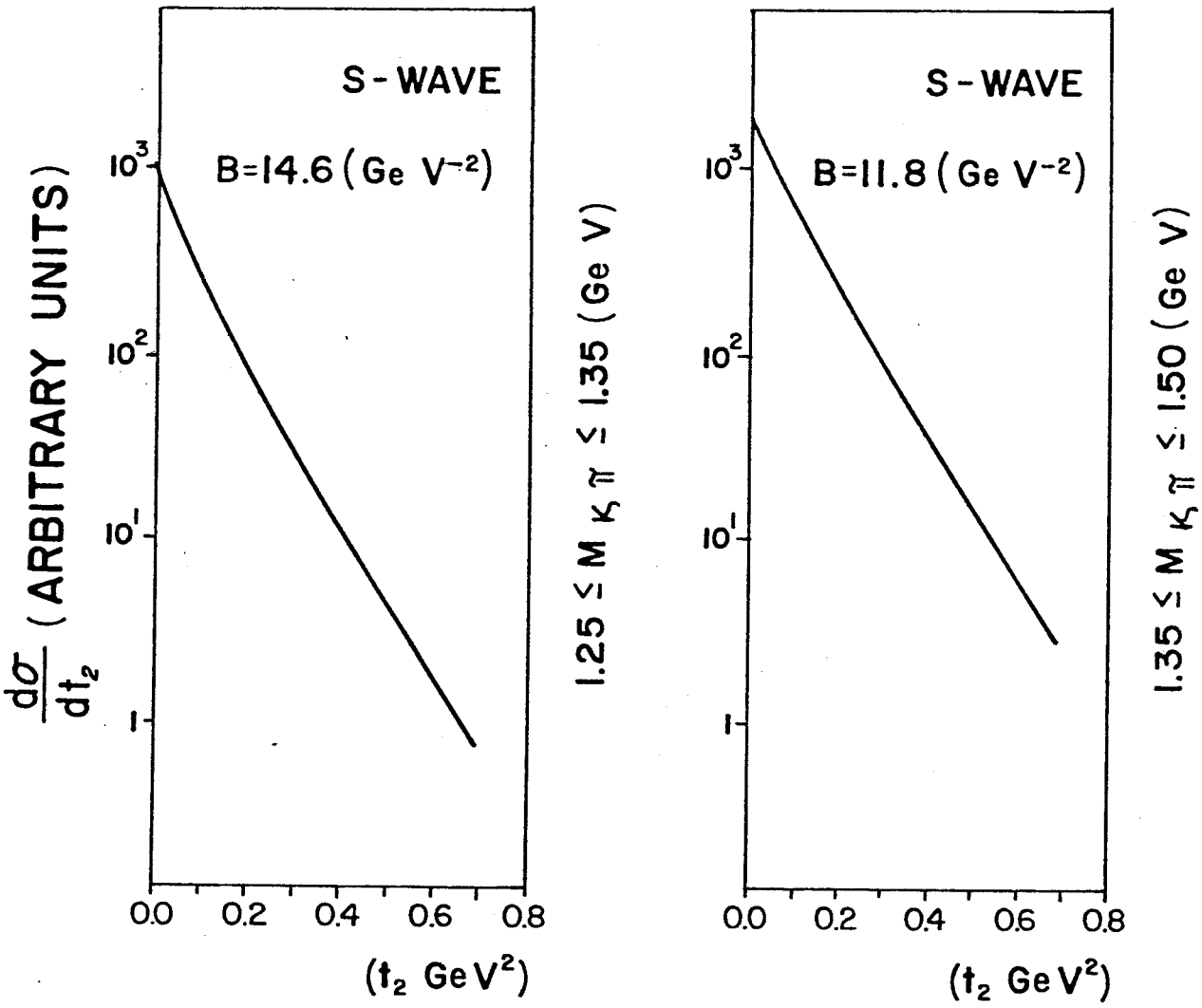
S-WAVE
B=14.6 (Ge V^{-2})
$\frac{d\sigma}{dt_2}$ (ARBITRARY UNITS)
10^3
10^2
10^1
1
0.0
0.2
0.4
0.6
0.8
(t_2 GeV^2)
1.25 ≤ M $_{K\pi}$ ≤ 1.35 (Ge V)
S-WAVE
B=11.8 (Ge V^{-2})
10^3
10^2
10^1
1
0.0
0.2
0.4
0.6
0.8
(t_2 GeV^2)
1.35 ≤ M $_{K\pi}$ ≤ 1.50 (Ge V)

Fig. 4

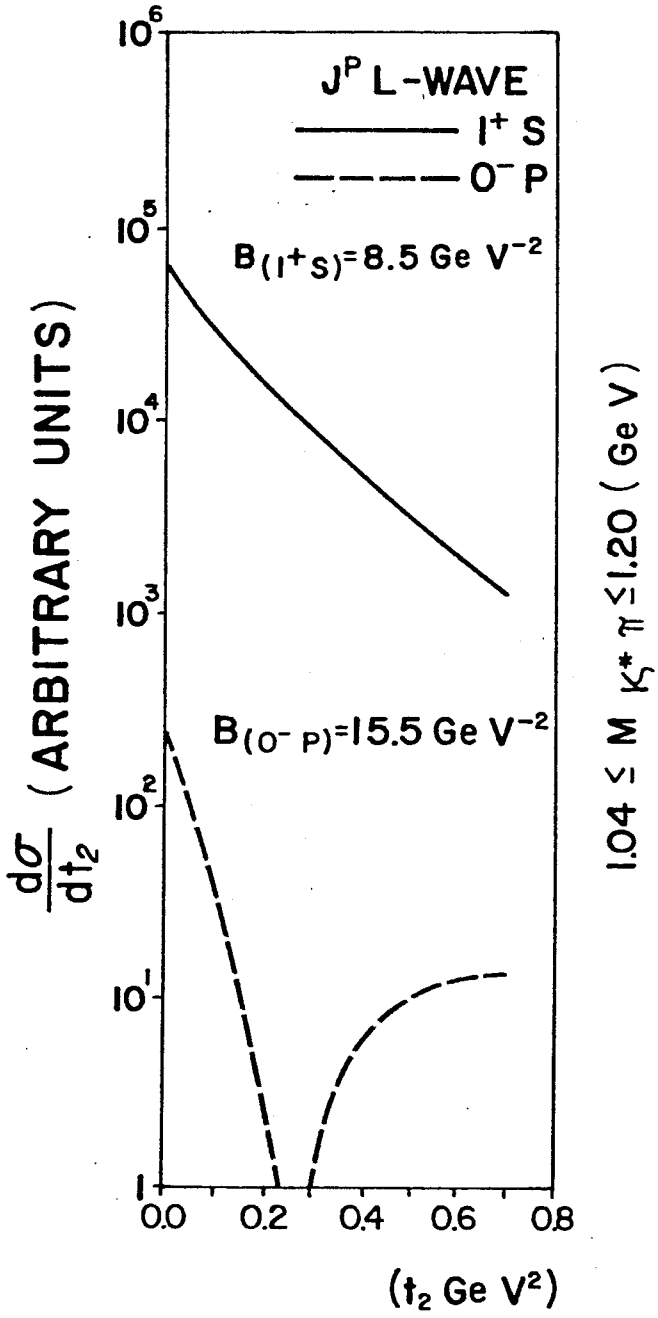
10^6
10^5
10^4
10^3
10^2
10^1
1
J^P L-WAVE
1^+ S
0^- P
$B_{(1^+S)}$=8.5 Ge V^{-2}
$B_{(0^- P)}$=15.5 Ge V^{-2}
$\frac{d\sigma}{dt_2}$ (ARBITRARY UNITS)
0.0
0.2
0.4
0.6
0.8
(t_2 Ge V^2)
1.04 ≤ M $K^*\pi$ ≤1.20 (Ge V)

Fig. 5

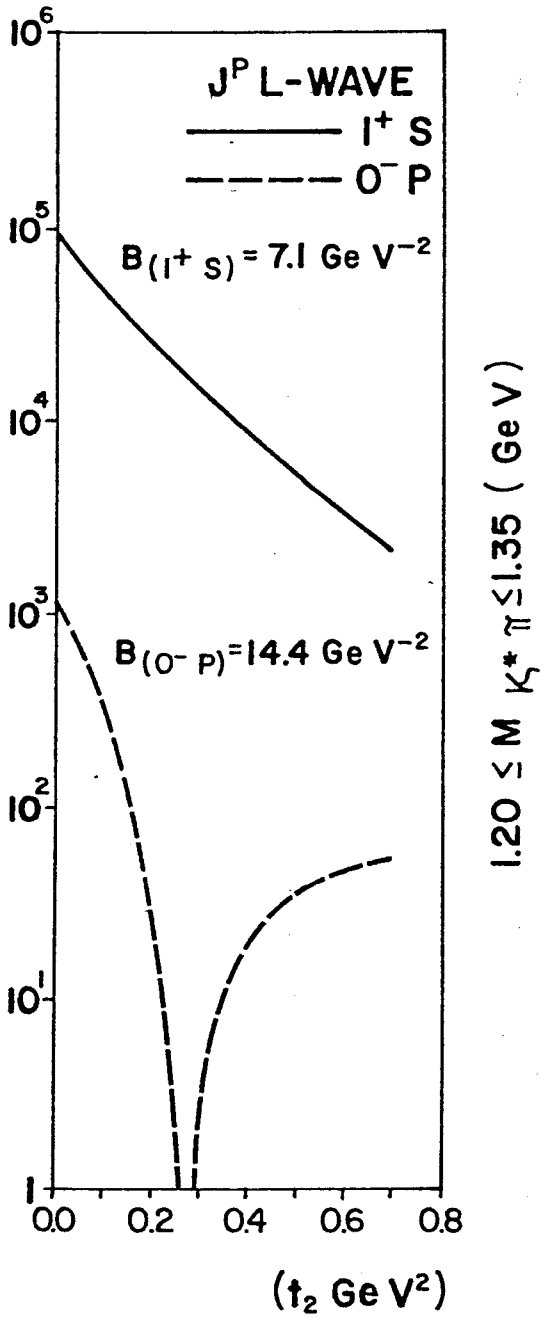
10^6
10^5
10^4
10^3
10^2
10^1
1
J^P L-WAVE
1^+ S
0^- P
$B_{(1^+S)}$ = 7.1 Ge V^{-2}
$B_{(0^- P)}$=14.4 Ge V^{-2}
0.0
0.2
0.4
0.6
0.8
(t_2 Ge V^2)
1.20 ≤ M $K^*\pi$ ≤1.35 (Ge V)

Fig. 6

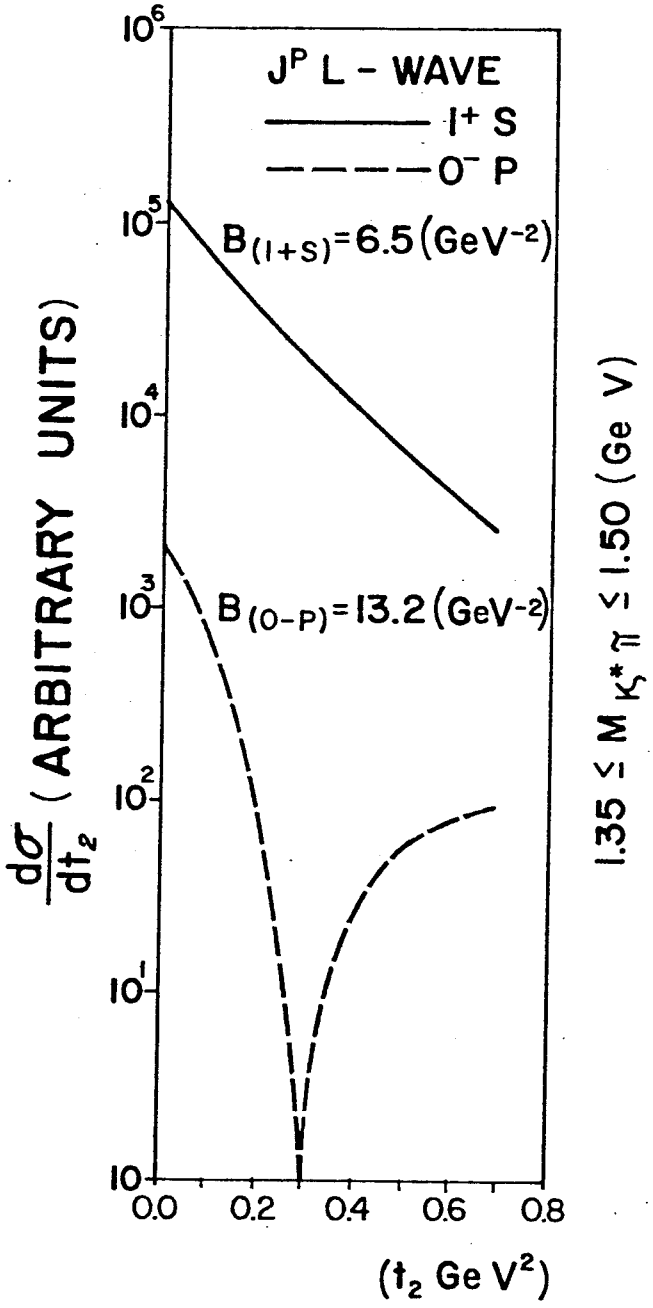
J^P L - WAVE
1^+ S
0^- P
$B_{(1+S)}=6.5\,(GeV^{-2})$
$B_{(0-P)}=13.2\,(GeV^{-2})$
$\frac{d\sigma}{dt_2}$ (ARBITRARY UNITS)
10^6
10^5
10^4
10^3
10^2
10^1
10
0.0
0.2
0.4
0.6
0.8
$(t_2\ GeV^2)$
$1.35 \leq M_{K^*\pi} \leq 1.50$ (Ge V)

Fig. 7

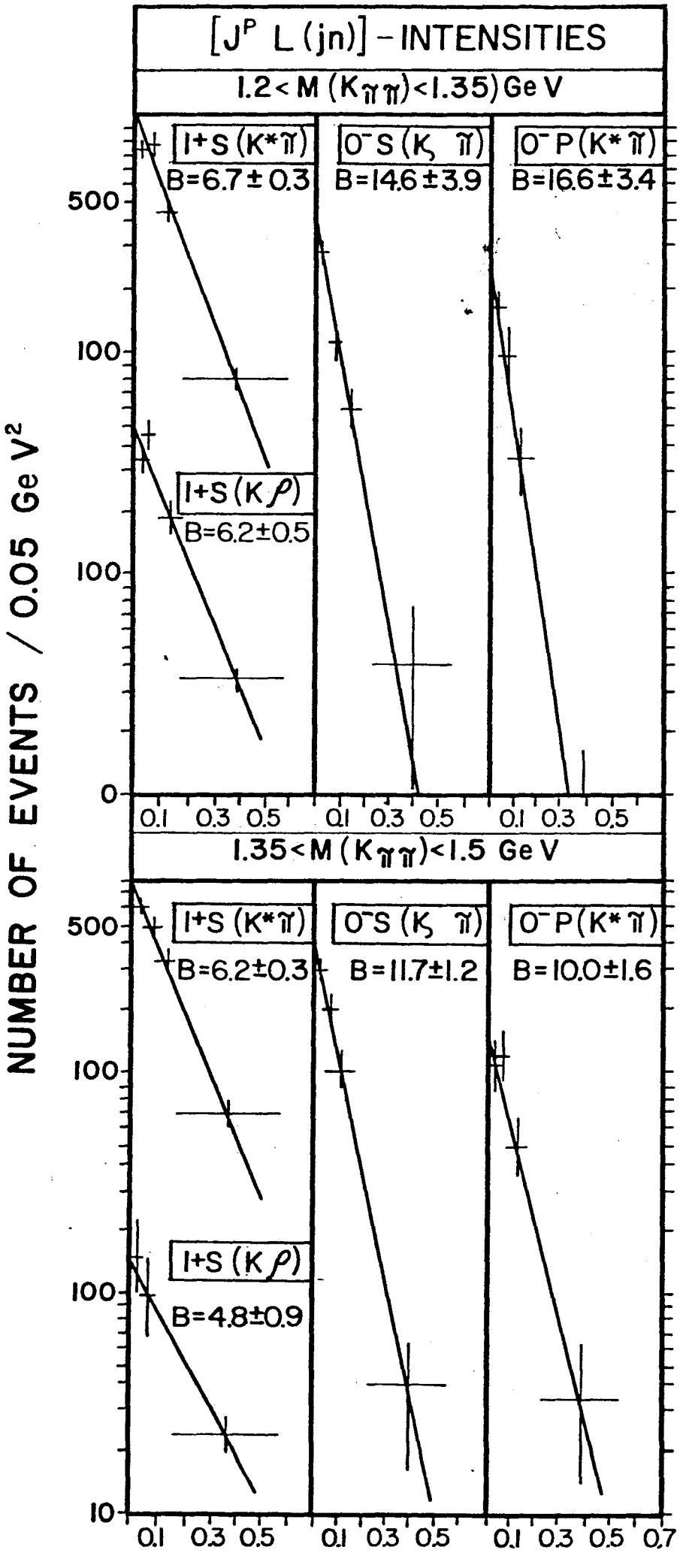
[J^P L (jn)] - INTENSITIES
1.2 < M (Kππ) < 1.35) Ge V
1+S (K*π)
B=6.7 ± 0.3
0⁻S (Kζ π)
B=14.6 ±3.9
0⁻P (K*π)
B=16.6±3.4
1+S (Kρ)
B=6.2±0.5
1.35 < M (Kππ) < 1.5 Ge V
1+S (K*π)
B=6.2±0.3
0⁻S (Kζ π)
B=11.7±1.2
0⁻P (K*π)
B=10.0±1.6
1+S (Kρ)
B=4.8±0.9
NUMBER OF EVENTS / 0.05 Ge V²
500
100
0
10
0.1 0.3 0.5 0.7

Fig. 8

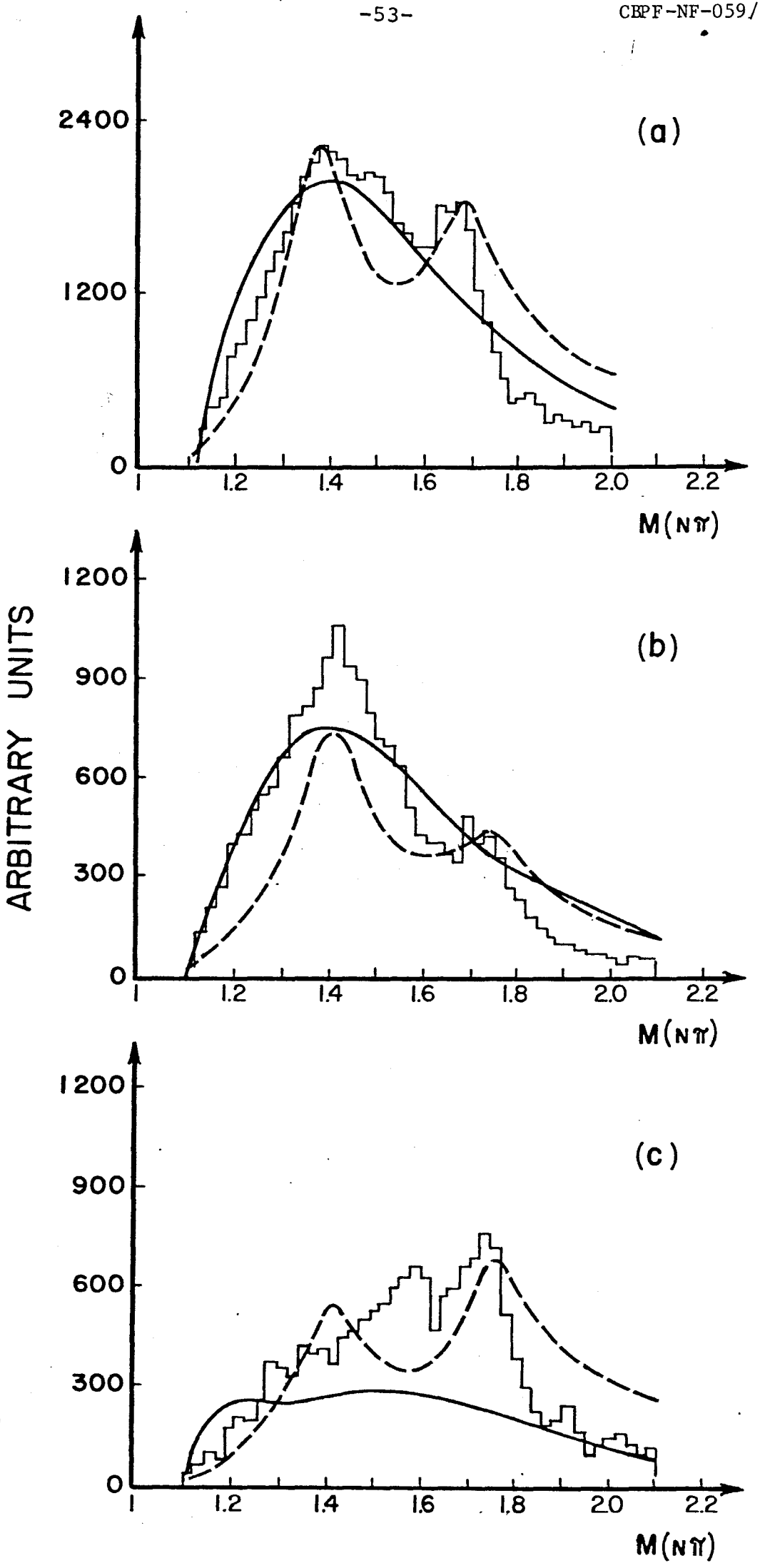
2400
1200
0
(a)
1.2
1.4
1.6
1.8
2.0
2.2
M(Nπ)
ARBITRARY UNITS
1200
900
600
300
0
(b)
1.2
1.4
1.6
1.8
2.0
2.2
M(Nπ)
1200
900
600
300
0
(c)
1.2
1.4
1.6
1.8
2.0
2.2
M(Nπ)

Fig. 9

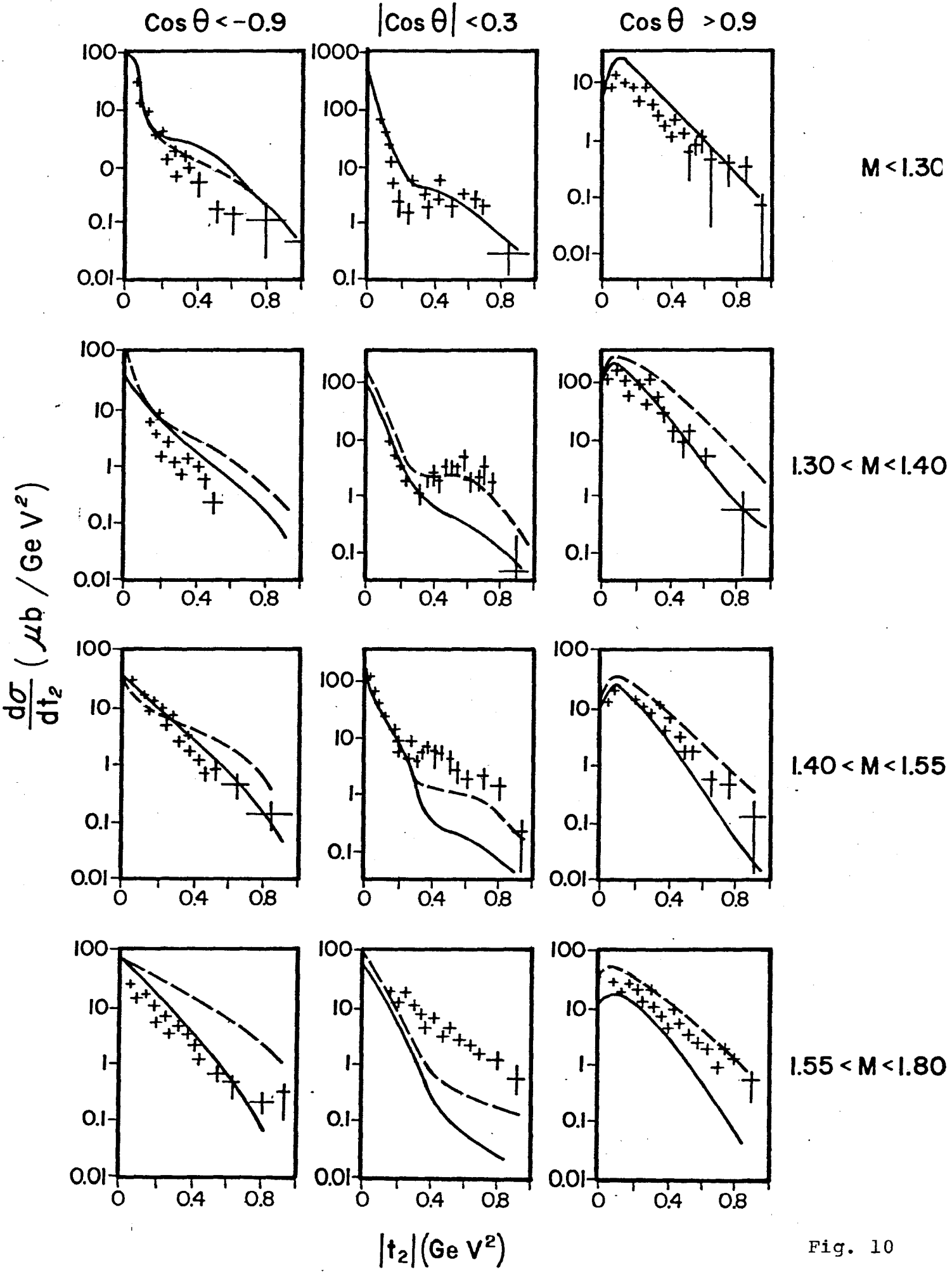
Cos θ < -0.9
|Cos θ| < 0.3
Cos θ > 0.9
M < 1.30
1.30 < M < 1.40
1.40 < M < 1.55
1.55 < M < 1.80
dσ/dt₂ (μb / Ge V²)
|t₂| (Ge V²)

Fig. 10

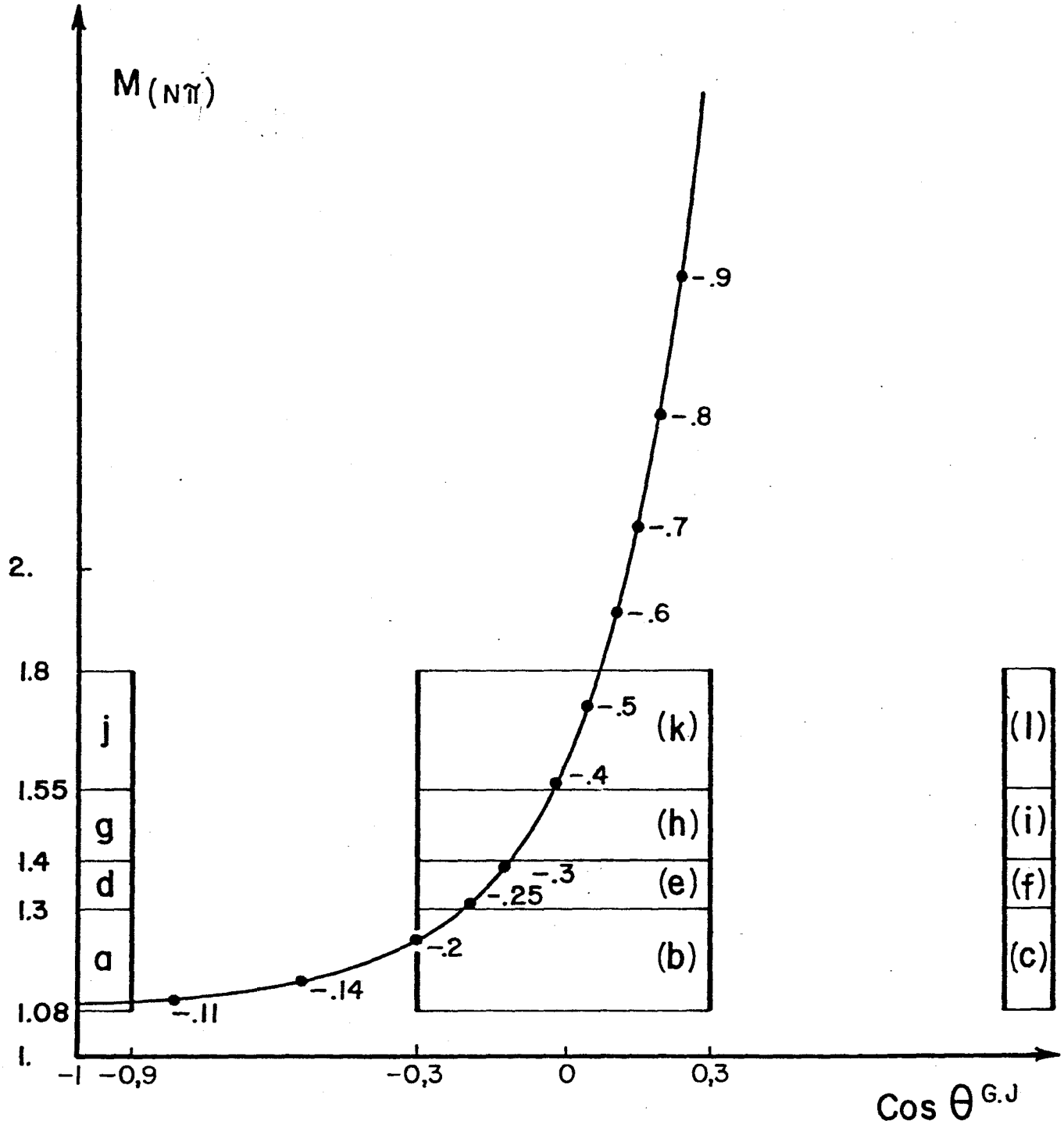
M(Nπ)
2.
1.8
1.55
1.4
1.3
1.08
1.
j
g
d
a
(k)
(h)
(e)
(b)
(l)
(i)
(f)
(c)
-.9
-.8
-.7
-.6
-.5
-.4
-.3
-.25
-.2
-.14
-.11
-1
-0,9
-0,3
0
0,3
Cos θ G.J

Fig. 11

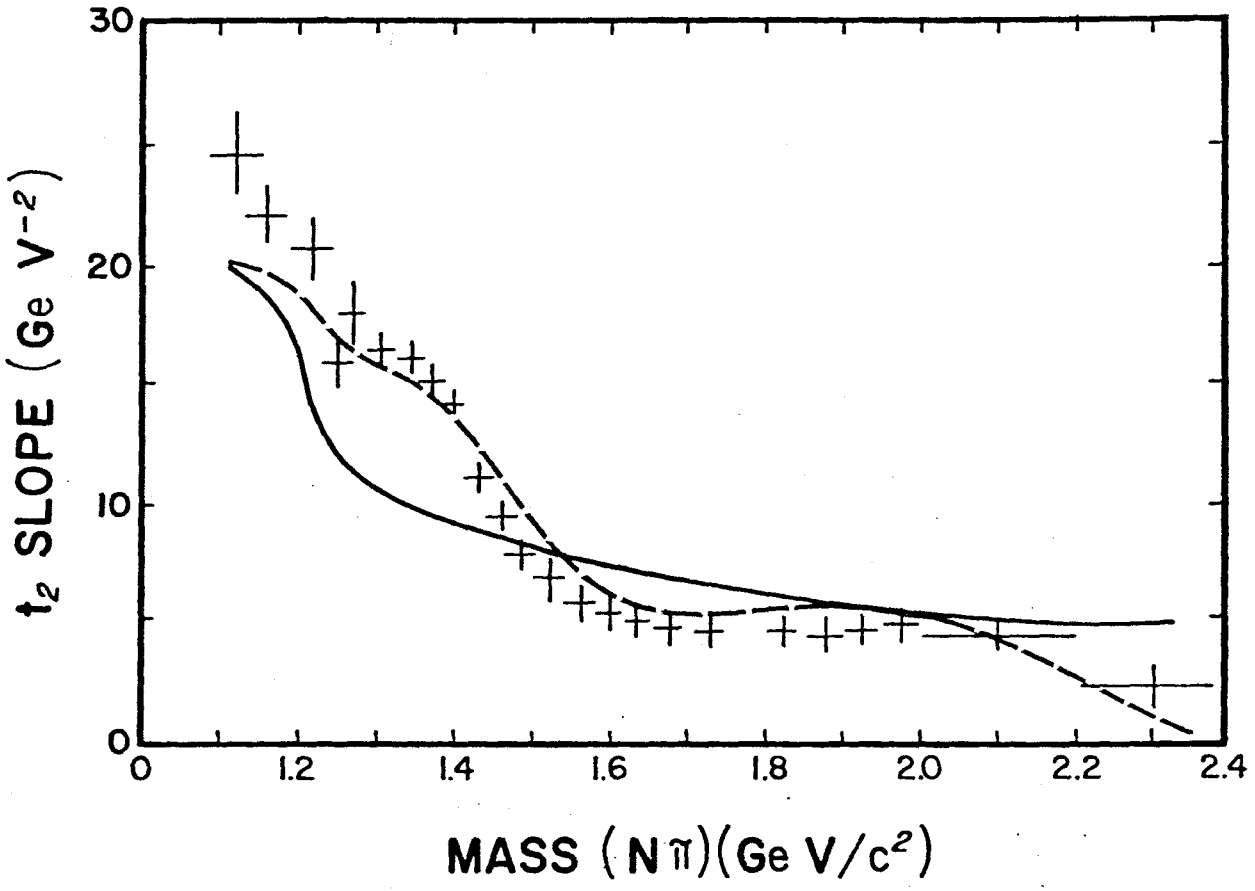

Fig. 12

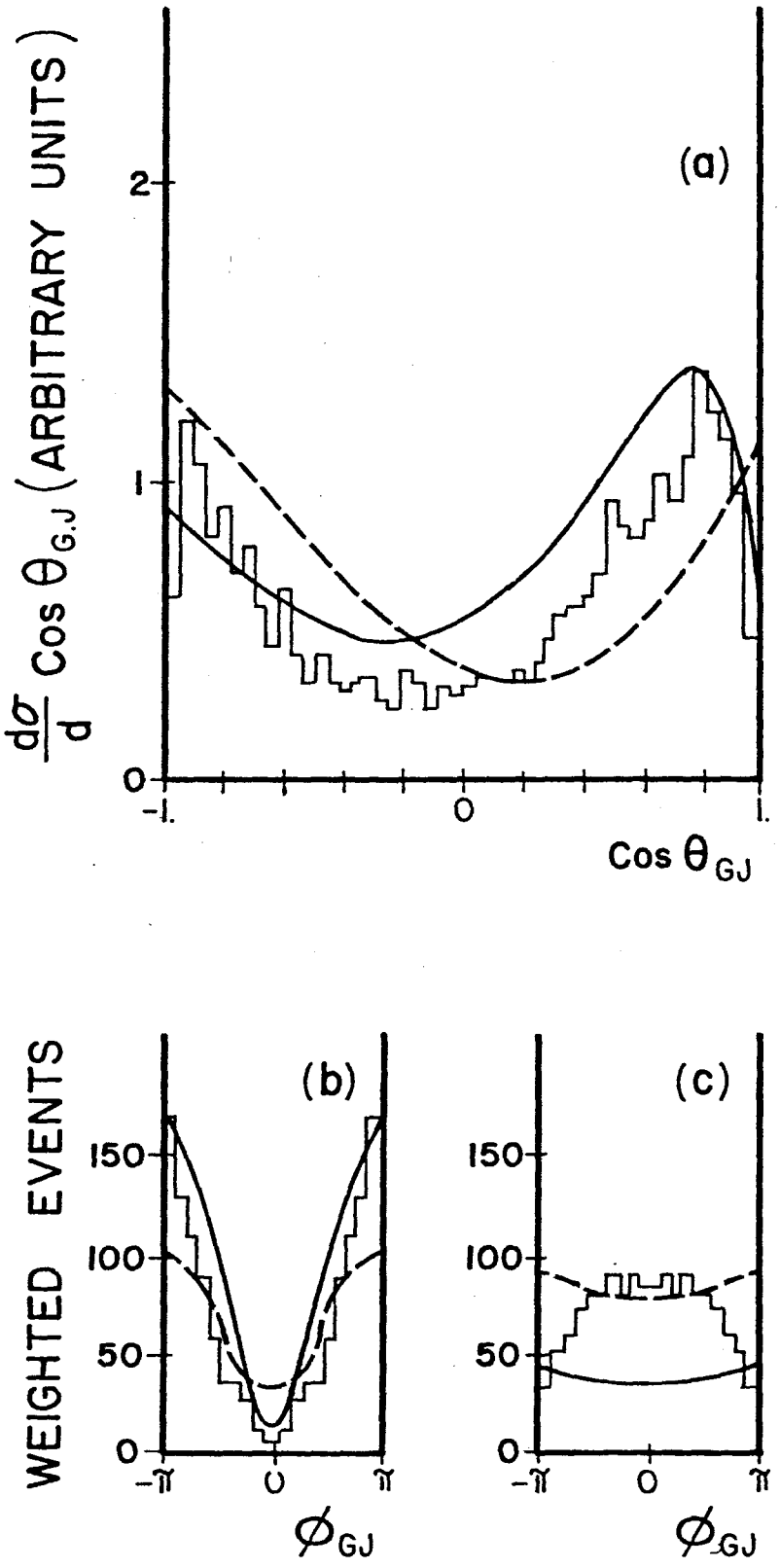
(a)
$\frac{d\sigma}{d}$ Cos $\theta_{G.J}$ (ARBITRARY UNITS)
2
1
0
-1.
0
1.
Cos θ_{GJ}
(b)
(c)
WEIGHTED EVENTS
150
100
50
0
$-\pi$
0
π
ϕ_{GJ}

Fig. 13

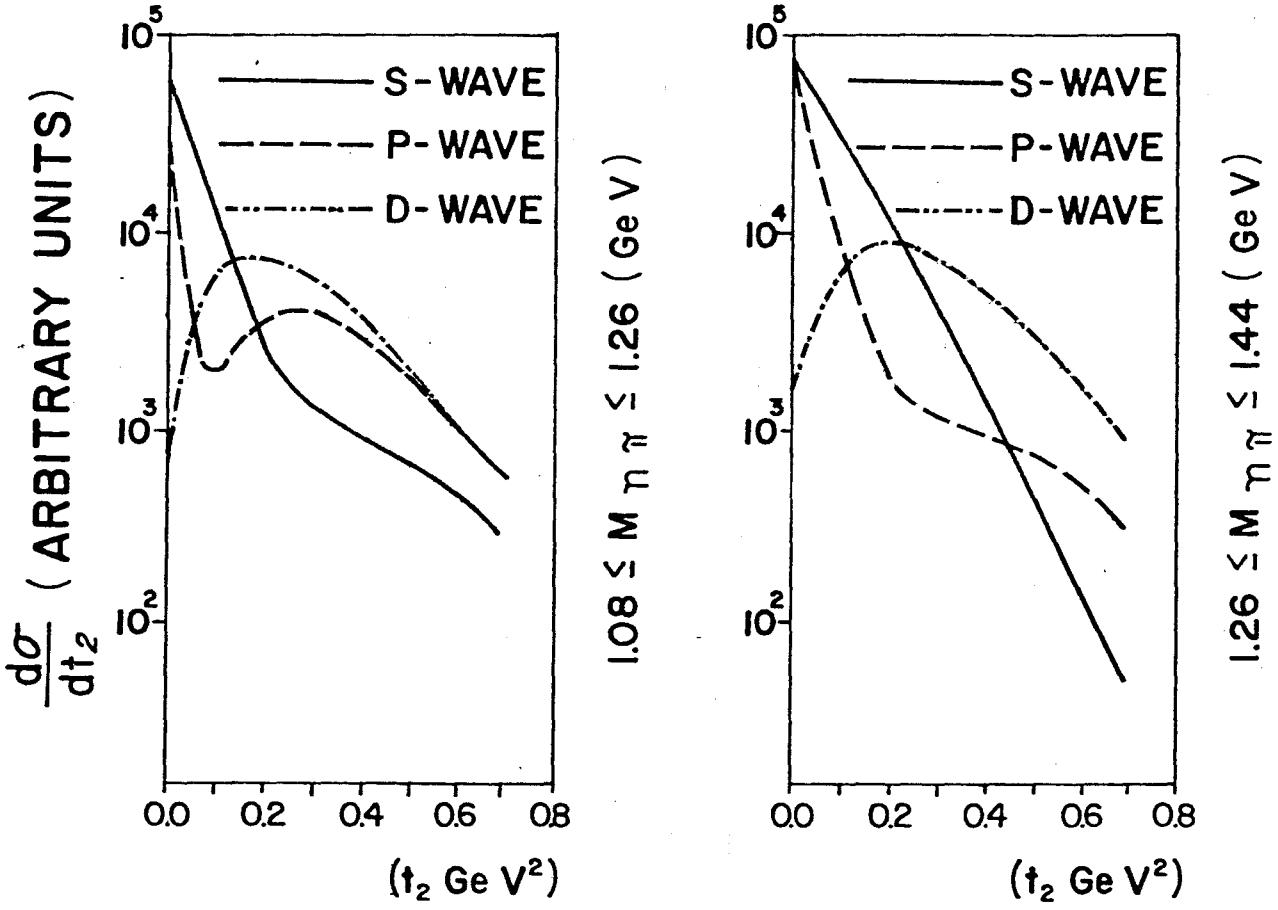
$\frac{d\sigma}{dt_2}$ (ARBITRARY UNITS)
10^5
10^4
10^3
10^2
S-WAVE
P-WAVE
D-WAVE
0.0
0.2
0.4
0.6
0.8
(t_2 Ge V^2)
1.08 ≤ M $\eta\pi$ ≤ 1.26 (Ge V)
1.26 ≤ M $\eta\pi$ ≤ 1.44 (Ge V)

Fig. 14

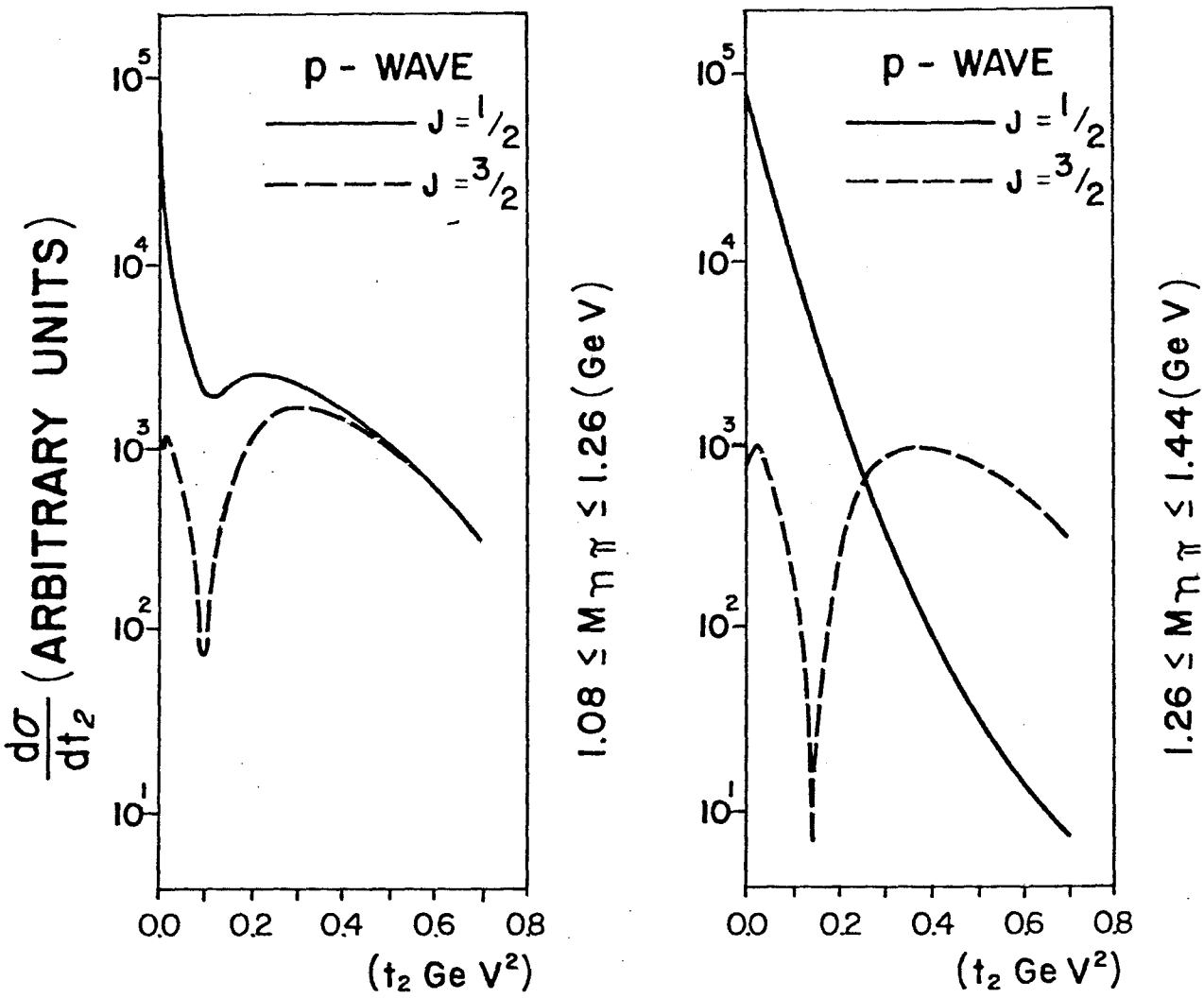
p - WAVE
J = 1/2
J = 3/2
$\frac{d\sigma}{dt_2}$ (ARBITRARY UNITS)
10^5
10^4
10^3
10^2
10^1
0.0
0.2
0.4
0.6
0.8
(t_2 Ge V^2)
1.08 ≤ M$\eta\pi$ ≤ 1.26 (Ge V)
p - WAVE
J = 1/2
J = 3/2
1.26 ≤ M$\eta\pi$ ≤ 1.44 (Ge V)

Fig. 15

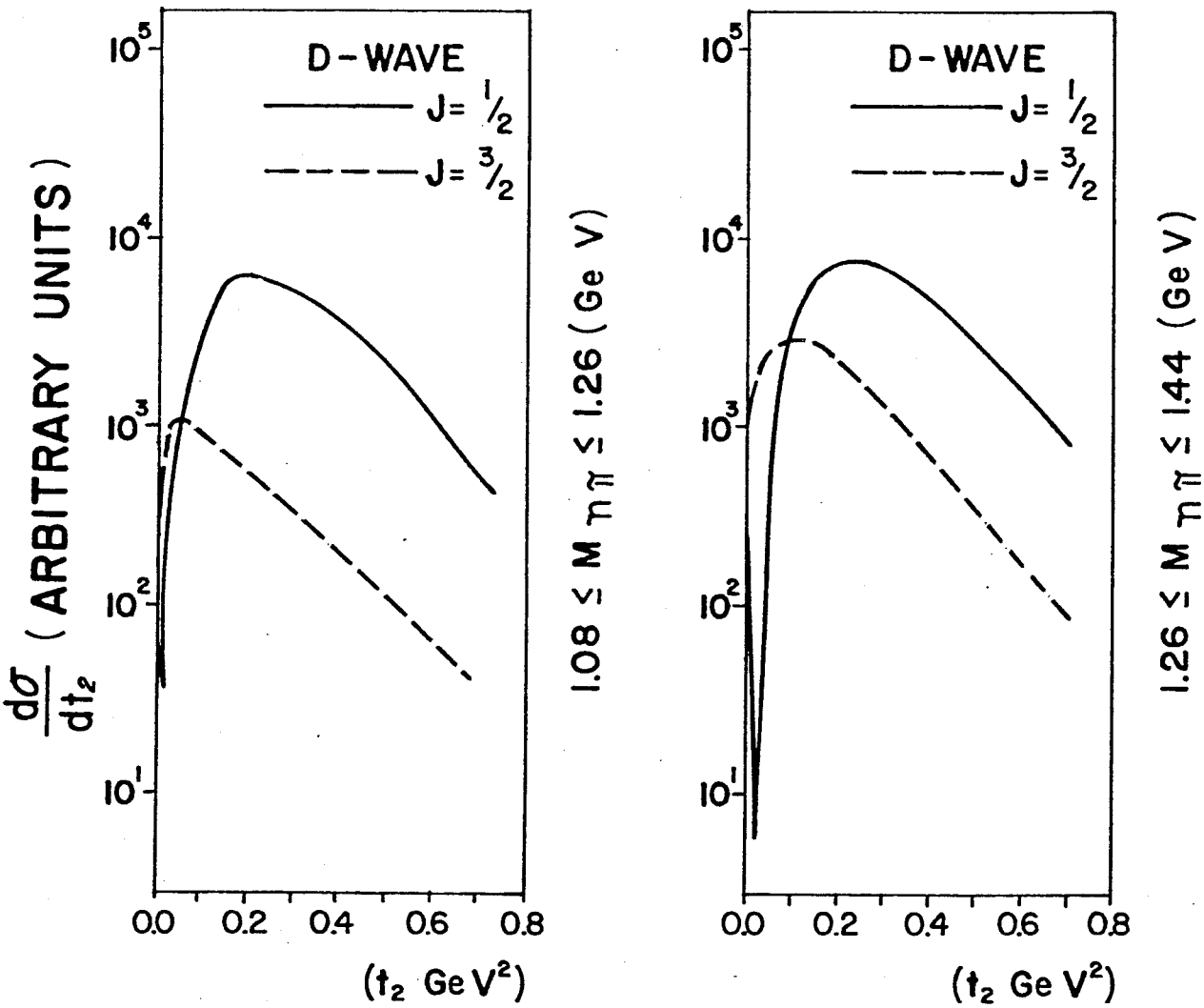
D-WAVE
J= 1/2
J= 3/2
$\frac{d\sigma}{dt_2}$ (ARBITRARY UNITS)
10^5
10^4
10^3
10^2
10^1
0.0
0.2
0.4
0.6
0.8
(t_2 GeV^2)
1.08 ≤ M $\eta\pi$ ≤ 1.26 (GeV)
D-WAVE
J= 1/2
J= 3/2
1.26 ≤ M $\eta\pi$ ≤ 1.44 (GeV)

Fig. 16

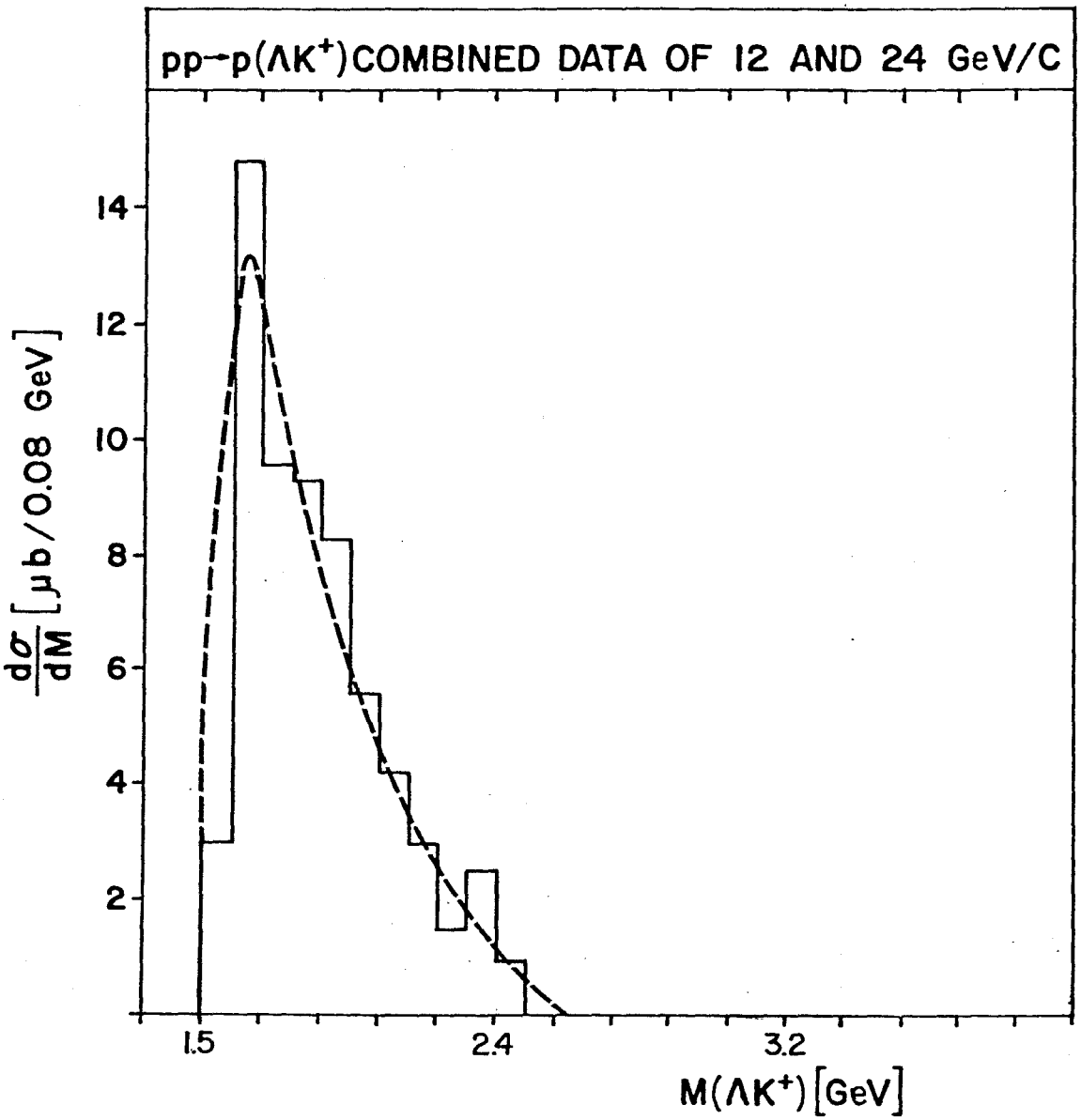
pp→p(ΛK⁺)COMBINED DATA OF 12 AND 24 GeV/C
dσ/dM [μb/0.08 GeV]
14
12
10
8
6
4
2
1.5
2.4
3.2
M(ΛK⁺) [GeV]

Fig. 17

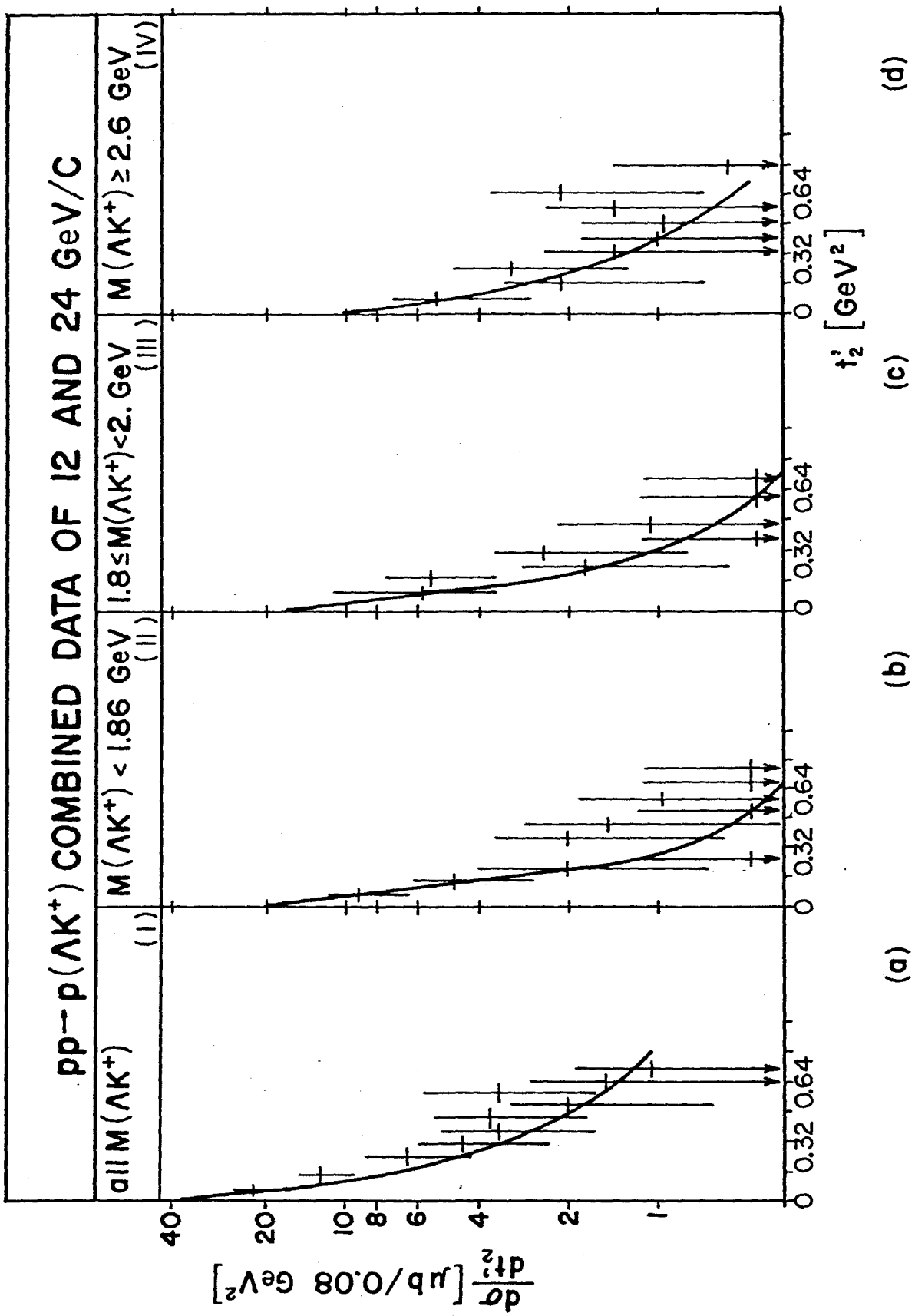
pp→p(ΛK⁺) COMBINED DATA OF 12 AND 24 GeV/C
all M(ΛK⁺)
(I)
M(ΛK⁺) < 1.86 GeV
(II)
1.8≤M(ΛK⁺)<2. GeV
(III)
M(ΛK⁺)≥ 2.6 GeV
(IV)
(a)
(b)
(c)
(d)
t'₂ [GeV²]
0
0.32
0.64
dσ/dt'₂ [μb/0.08 GeV²]
40
20
10
8
6
4
2
1

Fig. 18

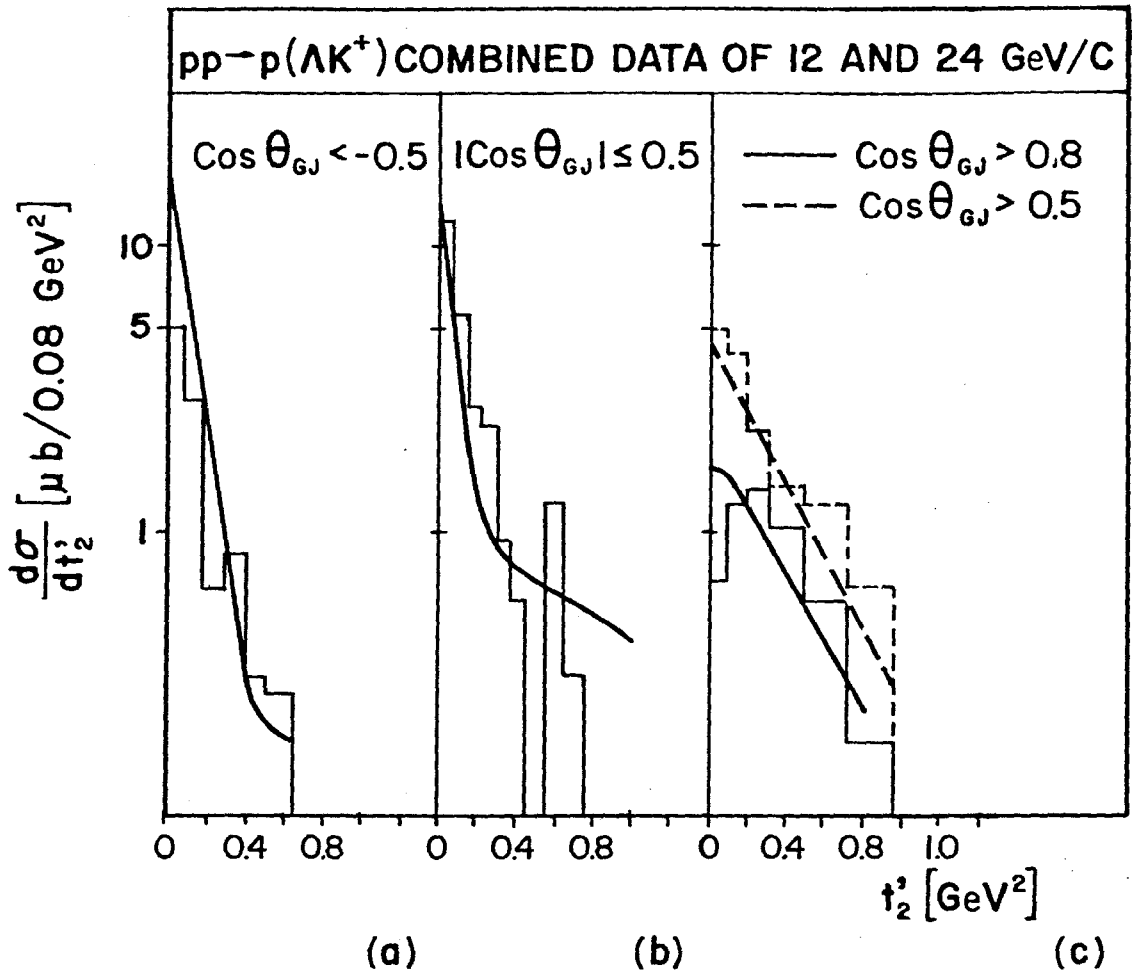
pp→p(ΛK+) COMBINED DATA OF 12 AND 24 GeV/C
Cos θGJ < -0.5
|Cos θGJ| ≤ 0.5
Cos θGJ > 0.8
Cos θGJ > 0.5
dσ/dt'2 [μb/0.08 GeV2]
10
5
1
0
0.4
0.8
1.0
t'2 [GeV2]
(a)
(b)
(c)

Fig. 19

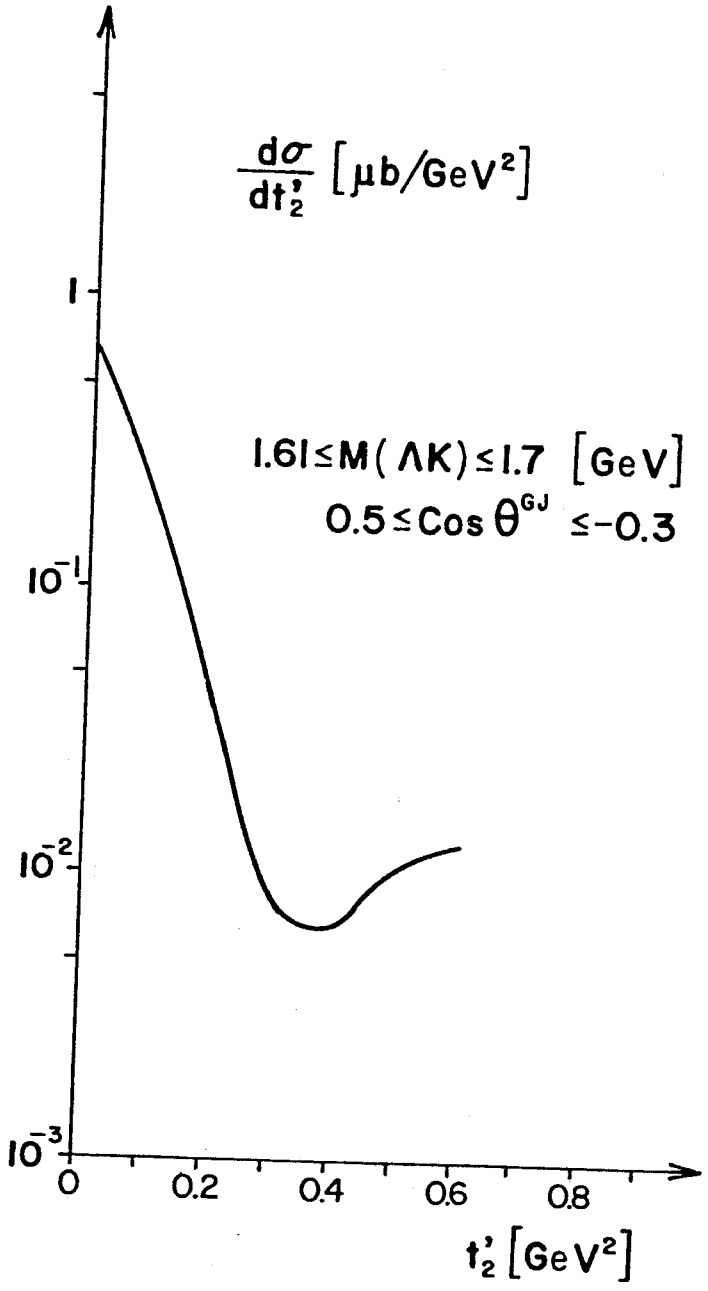
$\frac{d\sigma}{dt_2'}$ [μb/GeV²]
1
10^{-1}
10^{-2}
10^{-3}
1.61≤M(ΛK)≤1.7 [GeV]
0.5≤Cos θ^{GJ} ≤-0.3
0
0.2
0.4
0.6
0.8
t_2' [GeV²]

Fig. 20.a

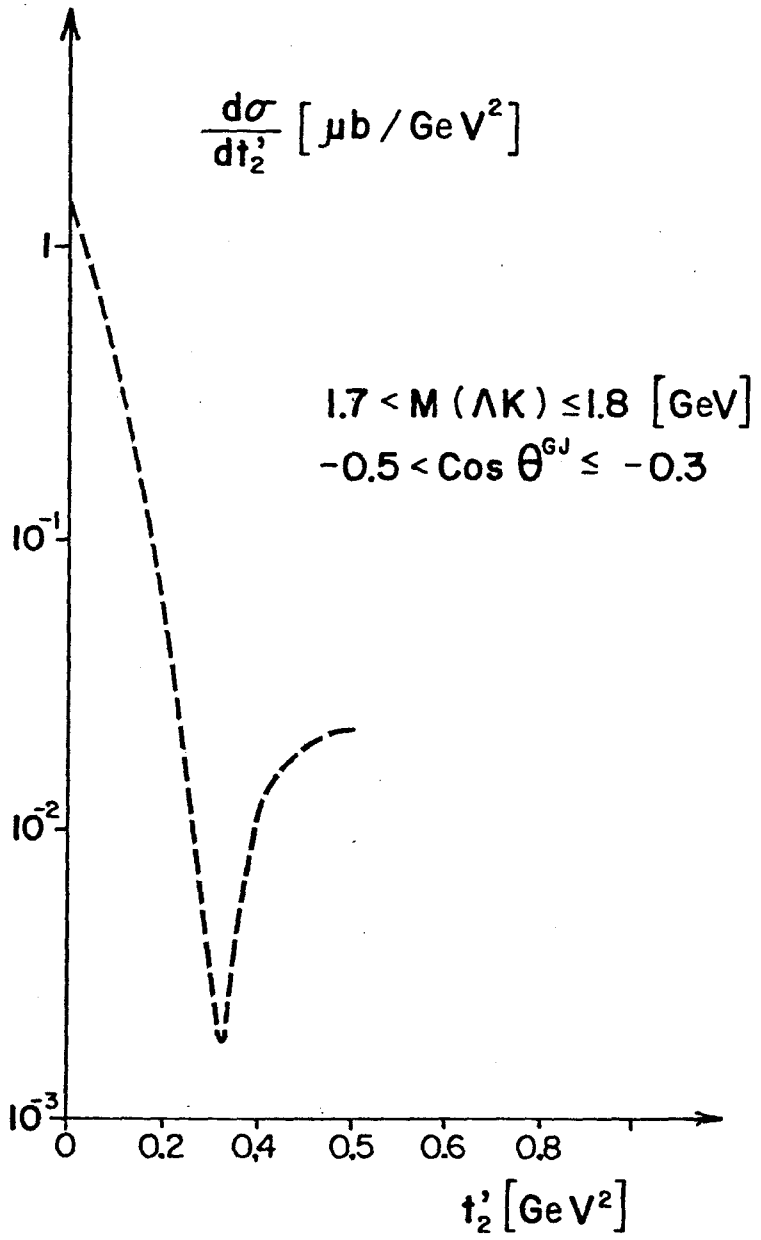
$\frac{d\sigma}{dt_2'}$ [μb / GeV²]
1
10^{-1}
10^{-2}
10^{-3}
0
0.2
0.4
0.5
0.6
0.8
t_2' [GeV²]
1.7 < M (ΛK) ≤ 1.8 [GeV]
-0.5 < Cos θ^{GJ} ≤ -0.3

Fig. 20.b

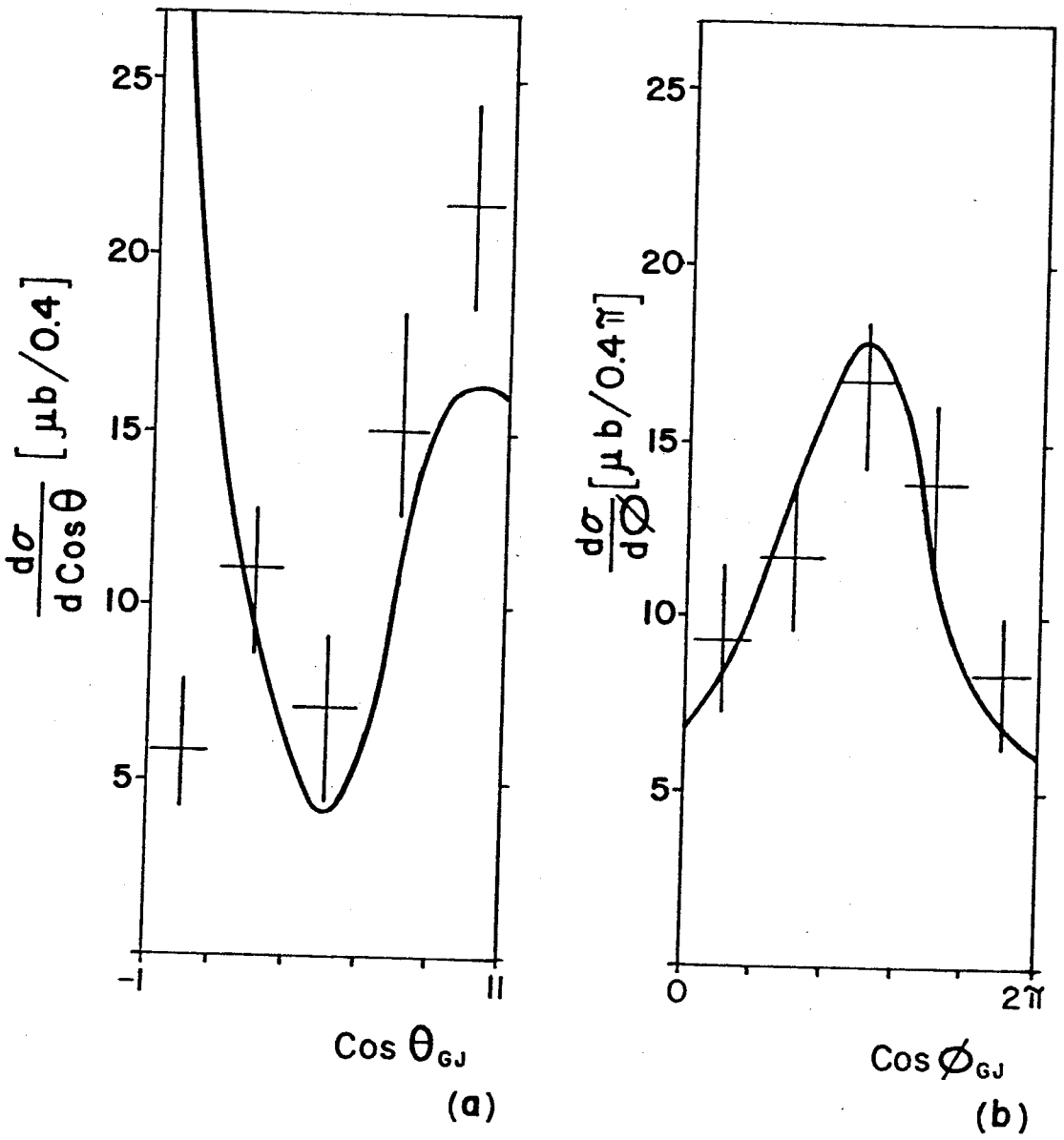
25
20
15
10
5
$\frac{d\sigma}{d\cos\theta}$ [μb/0.4]
-1
1
$\cos\theta_{GJ}$
(a)
25
20
15
10
5
$\frac{d\sigma}{d\phi}$[μb/0.4π]
0
2π
$\cos\phi_{GJ}$
(b)

Fig. 21

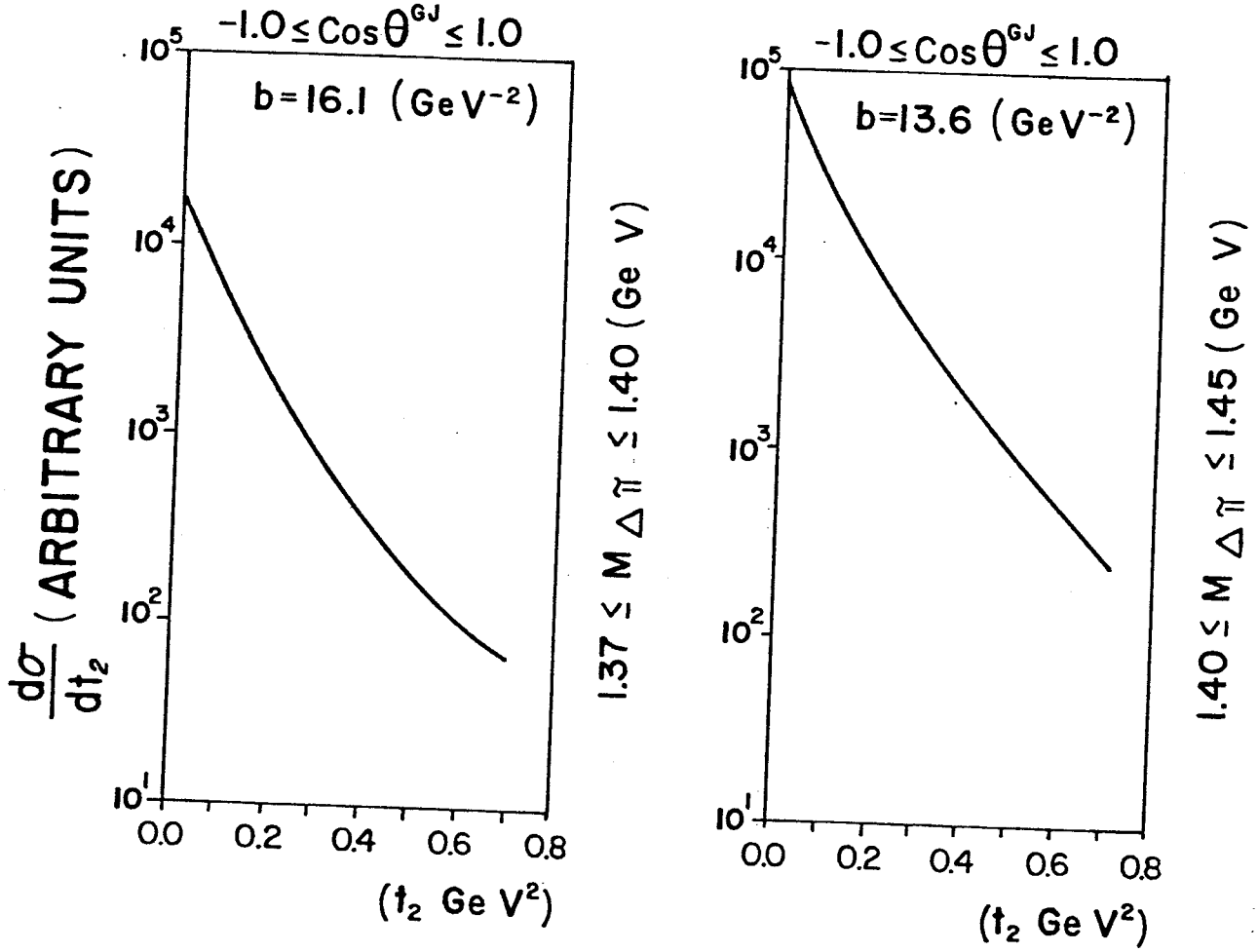
$-1.0 \leq \cos\theta^{GJ} \leq 1.0$
$b = 16.1\ (GeV^{-2})$
$\frac{d\sigma}{dt_2}$ (ARBITRARY UNITS)
10^5
10^4
10^3
10^2
10^1
0.0
0.2
0.4
0.6
0.8
$(t_2\ GeV^2)$
$1.37 \leq M_{\Delta\pi} \leq 1.40$ (Ge V)
$-1.0 \leq \cos\theta^{GJ} \leq 1.0$
$b = 13.6\ (GeV^{-2})$
$1.40 \leq M_{\Delta\pi} \leq 1.45$ (Ge V)

Fig. 22

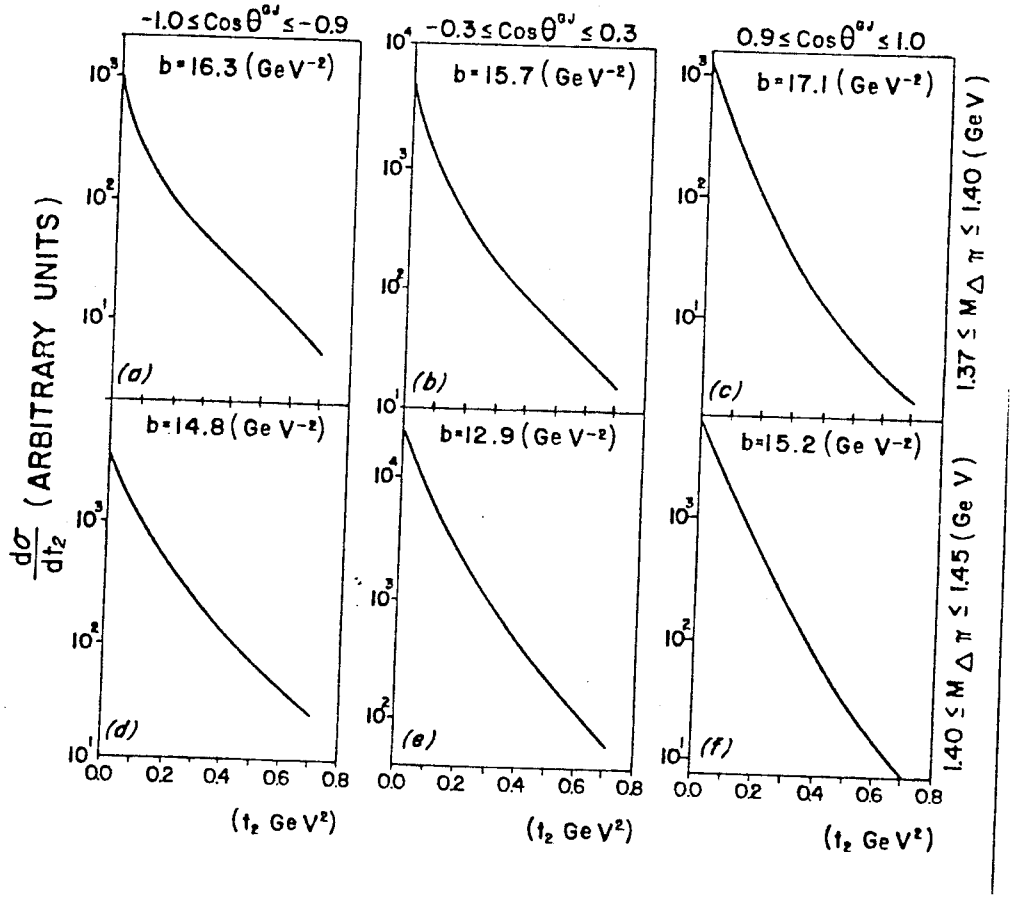
-1.0 ≤ Cos θ^GJ ≤ -0.9
-0.3 ≤ Cos θ^GJ ≤ 0.3
0.9 ≤ Cos θ^GJ ≤ 1.0
b = 16.3 (GeV^-2)
b = 15.7 (GeV^-2)
b = 17.1 (GeV^-2)
b = 14.8 (GeV^-2)
b = 12.9 (GeV^-2)
b = 15.2 (GeV^-2)
(a)
(b)
(c)
(d)
(e)
(f)
dσ/dt₂ (ARBITRARY UNITS)
(t₂ GeV²)
1.37 ≤ M Δ π ≤ 1.40 (GeV)
1.40 ≤ M Δ π ≤ 1.45 (GeV)

Fig. 23

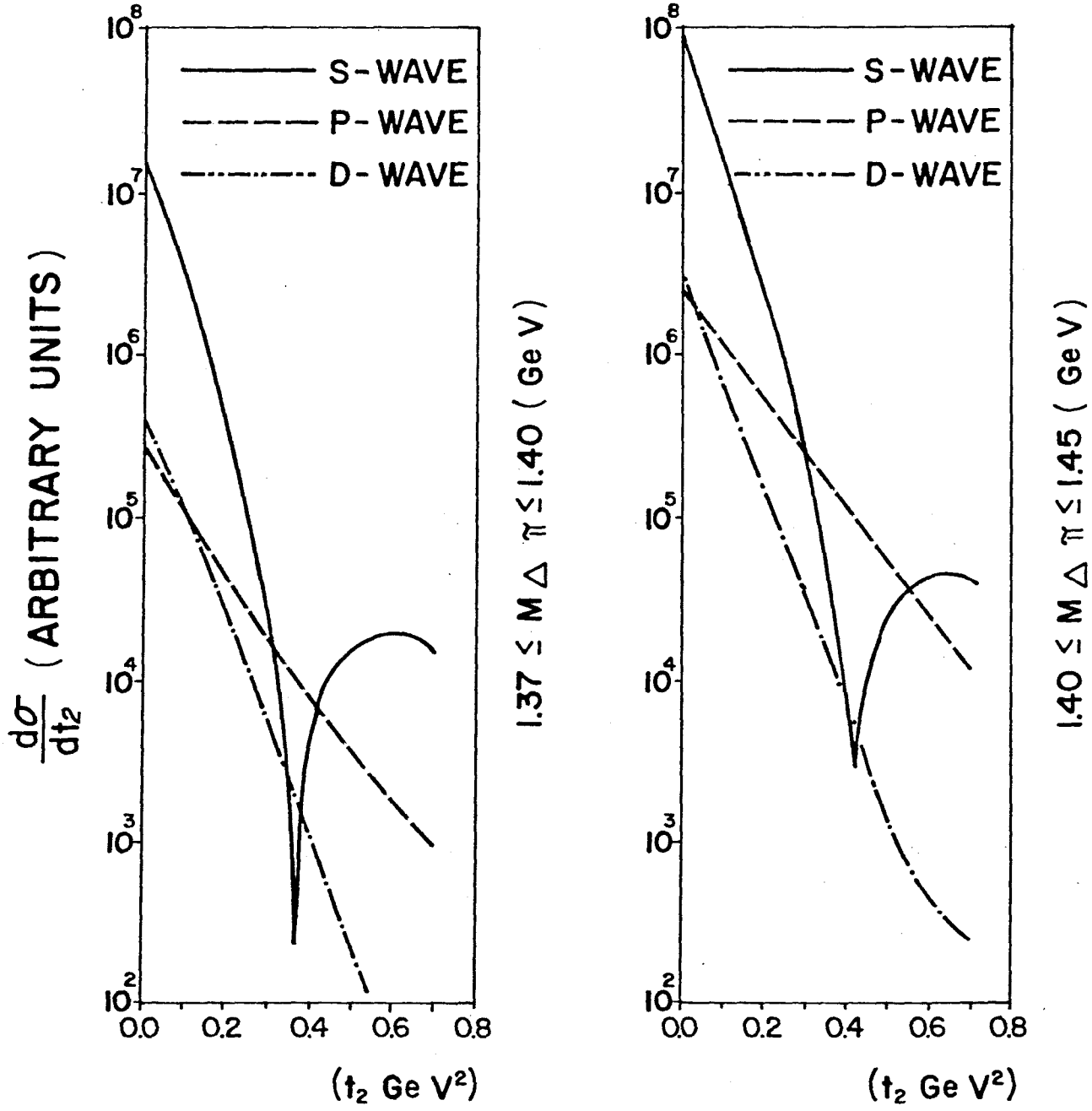
S-WAVE
P-WAVE
D-WAVE
$\frac{d\sigma}{dt_2}$ (ARBITRARY UNITS)
10^8
10^7
10^6
10^5
10^4
10^3
10^2
0.0
0.2
0.4
0.6
0.8
(t_2 Ge V^2)
$1.37 \leq M_{\Delta^{++}\pi^-} \leq 1.40$ (Ge V)
S-WAVE
P-WAVE
D-WAVE
10^8
10^7
10^6
10^5
10^4
10^3
10^2
0.0
0.2
0.4
0.6
0.8
(t_2 Ge V^2)
$1.40 \leq M_{\Delta^{++}\pi^-} \leq 1.45$ (Ge V)

Fig. 24

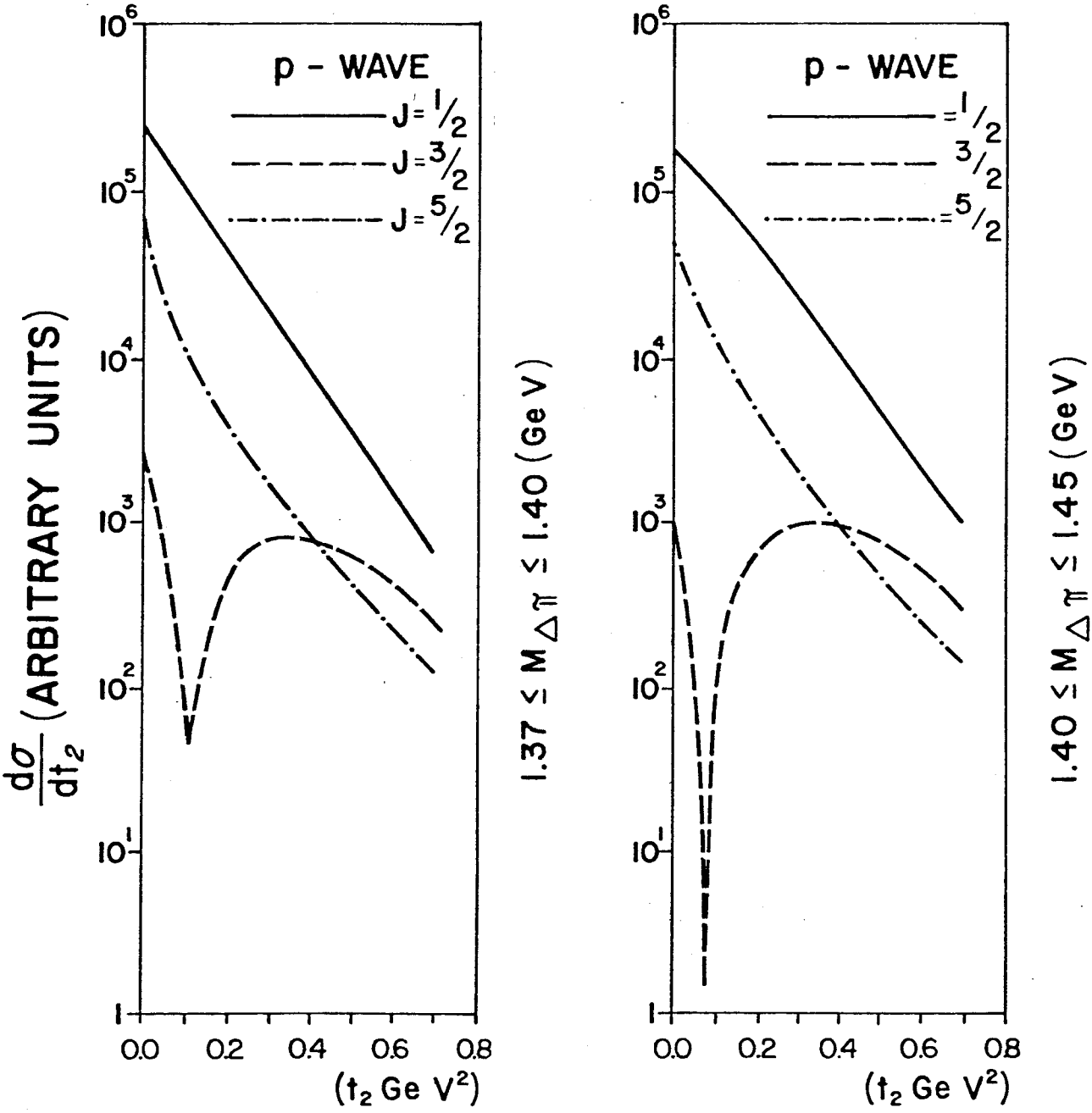
p - WAVE
J = 1/2
J = 3/2
J = 5/2
dσ/dt2 (ARBITRARY UNITS)
10^6
10^5
10^4
10^3
10^2
10^1
1
0.0
0.2
0.4
0.6
0.8
(t2 Ge V^2)
1.37 ≤ M Δπ ≤ 1.40 (Ge V)
p - WAVE
=1/2
3/2
=5/2
1.40 ≤ M Δπ ≤ 1.45 (Ge V)

Fig. 25

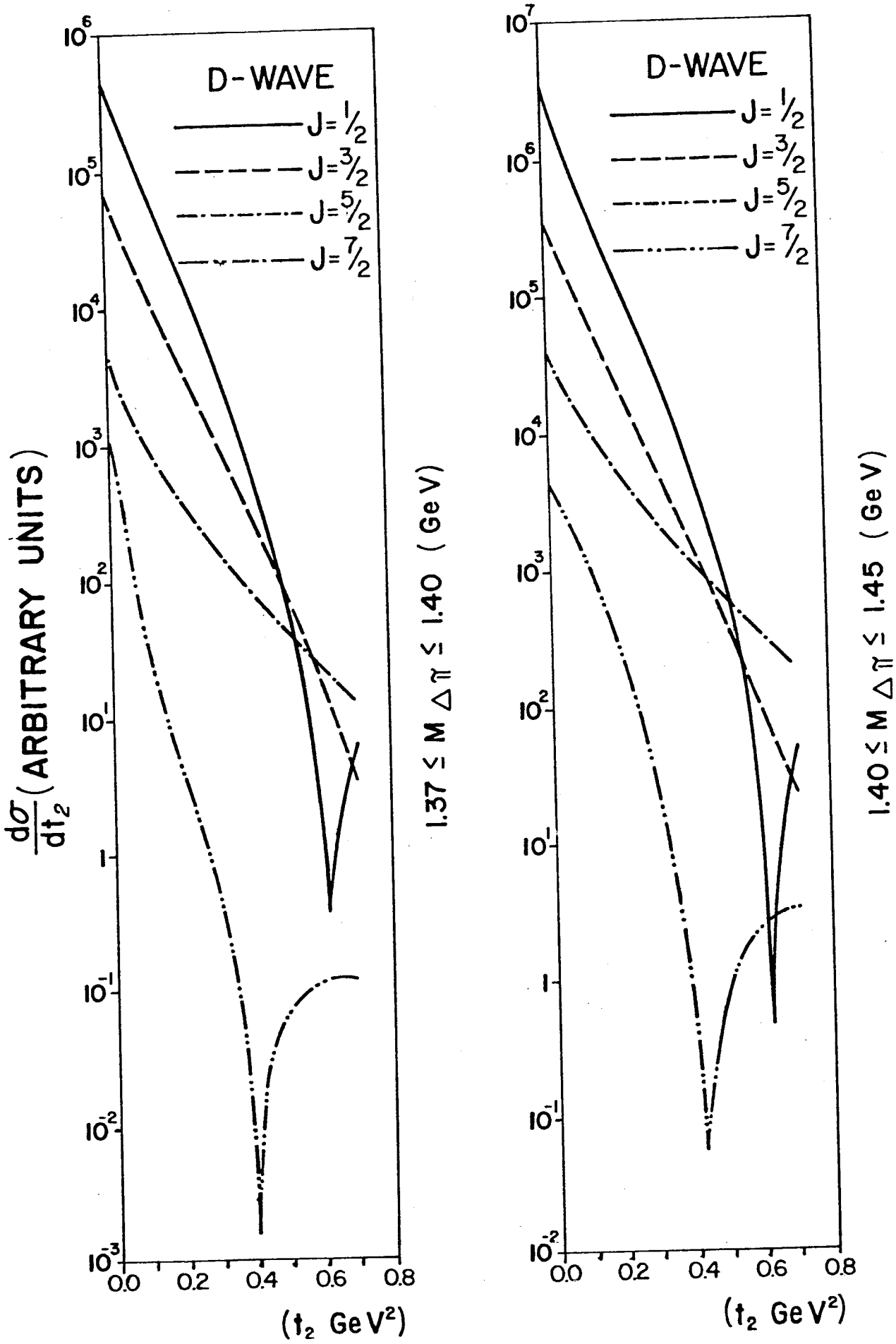
D-WAVE
J= 1/2
J=3/2
J=5/2
J=7/2
dσ/dt2 (ARBITRARY UNITS)
(t2 GeV2)
1.37 ≤ M Δπ ≤ 1.40 (GeV)
1.40 ≤ M Δπ ≤ 1.45 (GeV)

Fig. 26

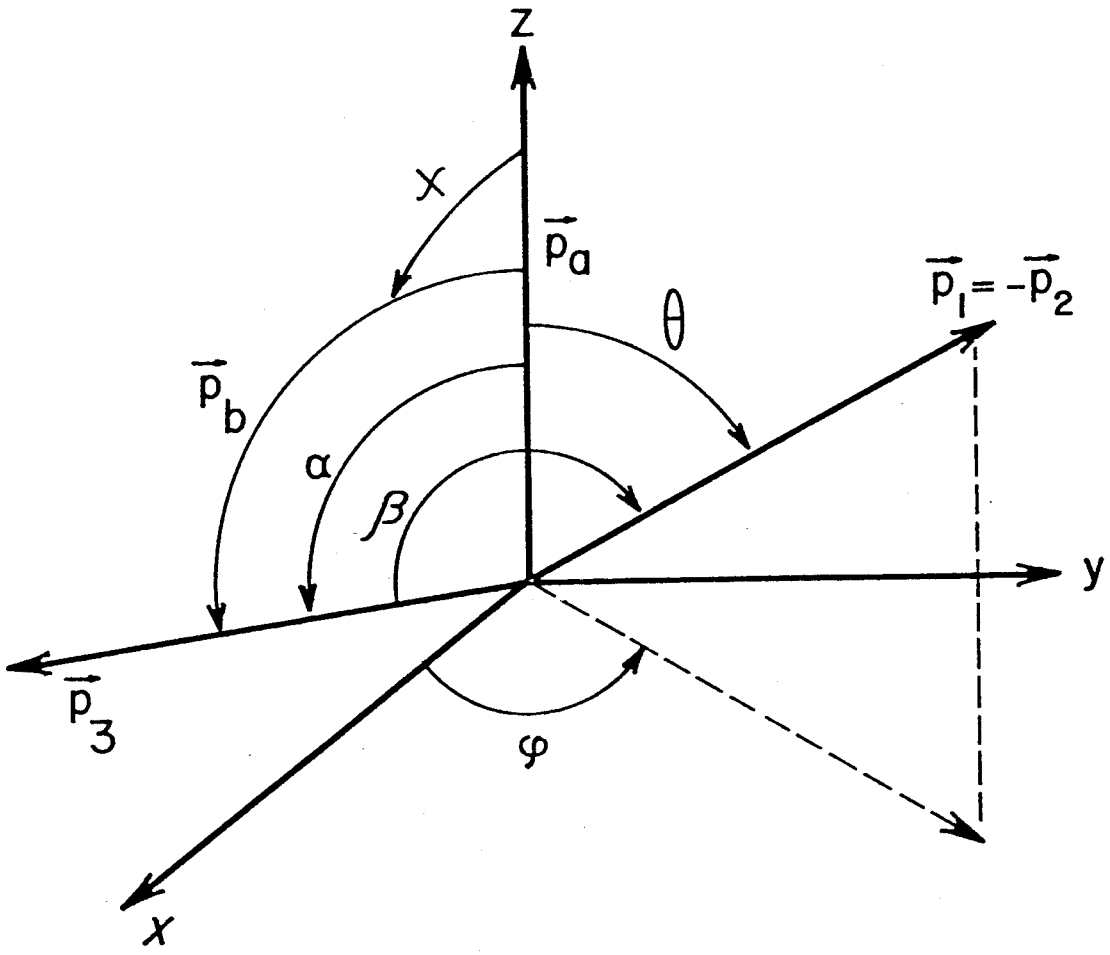

Fig. 27

REFERENCES

1. a) G. Cohen-Tannoudji, A. Santoro and M. Souza, N. Physics B125, 445 (1977)

   b) G. Cohen-Tannoudji, D. Levy and M. Souza -N. Phys. B129, 286 (1977)

   c) A. Endler, M.A.R. Monteiro, A. Santoro and M. Souza, Z. für Physik C7, 137 (1981)

   d) A.C.B. Antunes, A.F.S. Santoro and M.H.G. Souza. Rev. Bras. de Física 13, 415 (1983) and 13, 601 (1983)

2. G. Alberi and G. Goggi, Phys. Rep. 74 , 1 (1981)

3. a) D.R.O. Morrison, P. Lett. 22, 528 (1966) and P. Rev. 165, 1699 (1968)

   b) V.N. Gribov-Yad. Fiz.5, 197(1967); Sov. J. Nucl. Phys. 5, 138(1967)

4. G. Otter, Acta Physica Polonica B3, 809 (1972)

5. P.D.B. Collins and F.D. Gault, Nucl. Phys. B112, 483 (1976)

6. a) S.D. Drell and K. Hiida - Phys. Rev. Lett, 199 (1961)

   b) R.T. Deck - Phys. Rev. Lett. 13, 169 (1964)

   c) M. Ross and Y.Y. Yam - Phys. Rev. Lett. 19, 546 (1967)

7. a) C. Broll - Thesis - Université de Paris 7 (1976)

   b) J. Biel et al. Phys. Rev. Let. 36, 504, 507 (1976)

   c) See references in [1a] above.

8. G. otter et al. - Nucl. Phys. B106, 77, (1976)